Trends and Architecture of the Bluestone Formation Turbidites in Point Pleasant Park, Halifax, Nova Scotia

J. Adam Fraser

Acknowledgements

Abstract

In the Meguma Supergroup, a series of sandy and shaly intervals formed in a range of depositional environments from deltaic to deepwater. The Lower Ordovician Bluestone Formation in Point Pleasant Park on the Halifax Peninsula is part of the Halifax Group. Prior studies examined the regional geology, micropaleontology, and metamorphism but paid little attention to sedimentology of these outcrops, in part due to the metamorphic overprint that can obscure primary physical sedimentary structures. The goal of this project is to interpret the depositional environment of these sediments and understand their distribution and architecture. Data were collected at outcrops along the Northwest Arm, Black Rock Beach, the Battery, and Sailors' Memorial Road to investigate the geometry and architecture of the studied sections. Data collection includes measuring and logging sections, paleocurrent measurements from such features as tool marks and current ripples, petrographic analysis, scintillometer measurements to create synthetic gamma logs, LiDAR to develop 3D geological models in Polyworks and Petrel. The strata comprise mainly quartz, mica, zircon and tourmaline, and shows five lithofacies. These lithofacies make up a cyclic lithofacies association which is separated by sharp or scoured contacts. Scintillometer analysis showed no apparent relationship to lithology, likely due to the moderate metamorphism throughout the Meguma Supergroup. Interpretation suggested that the lithofacies association is characteristic of the Bouma sequence T_{a-e} and represents low density turbidites. Current ripples on bedding planes indicate the paleocurrent was towards the northwest. The beds fine and become thinner towards the top of the outcrop and lithofacies like meta sandy-siltstone ripples, and structureless silty slate to slate become more dominant, due to the reduction of sediment supply. Lithofacies and sedimentary structures seen in the outcrop, suggest these sediments were deposited from hypocynal turbidites on the distal overbank and levees of channels.

Key words: Fine-grained low density turbidites, Bouma sequence, Bluestone Formation, LiDAR, architecture, overbank and levee, Ordovician, Halifax Group, Point Pleasant Park.

Table of Contents

Chapters	**Page**

1.Introduction

1.1 Purpose of Study

The purpose of this study is to analyze the trends and architecture of Lower Ordovician Bluestone Formation sediments, interpreted as fine-grained turbidites in Point Pleasant Park.

Prior studies e.g Schenk (1975; 1997), Waldron (1987; 2009), Scott (2003), Tobey (2004) White (2009), Jamieson (2009), and Scallion (2010) examined the regional and structural geology, micropaleontology, and metamorphism but paid little attention to the sedimentology of the strata exposed in these outcrops, in part due to the metamorphic overprint that can obscure primary physical sedimentary structures.

This study provides insight into the depositional history of these sediments and provides an analogue for fine grained turbidite reservoirs that may be present in the subsurface offshore Nova Scotia and unconventional plays. This study also provides analogue models for exploration for high density turbidite flows that typically are more sand rich.

1.2 Study Area and General History

The study area (Fig. 1.1) is located in Point Pleasant Park on the Halifax Peninsula. This park covers an area of 75 hectares and is bounded to the east and south west by the Halifax Harbour and North West Arm opening to the Atlantic Ocean. The park is forested, with a rocky rim of beaches.

The park was originally used for hunting, and fishing by the M'kmaq people. It was a military battery for England in 1749 and continued as a military base through the two World Wars. The most recent event that affected Point Pleasant Park was

Hurricane Juan September 23 2003, which blew down and destroyed 2/3 of the trees and vegetation in the park. Today reforestation is restoring the park to the state before the storm.

1.3 Meguma Supergroup and Halifax Group

Mainland Nova Scotia is made up of two major supergroups; the Meguma (Fig. 1.1) and the Annapolis. The Meguma Supergroup ages range from Cambrian to the Lower Ordovician and is found on mainland Nova Scotia and is exposed along the coastal reaches of the province (Schenk, 1997).
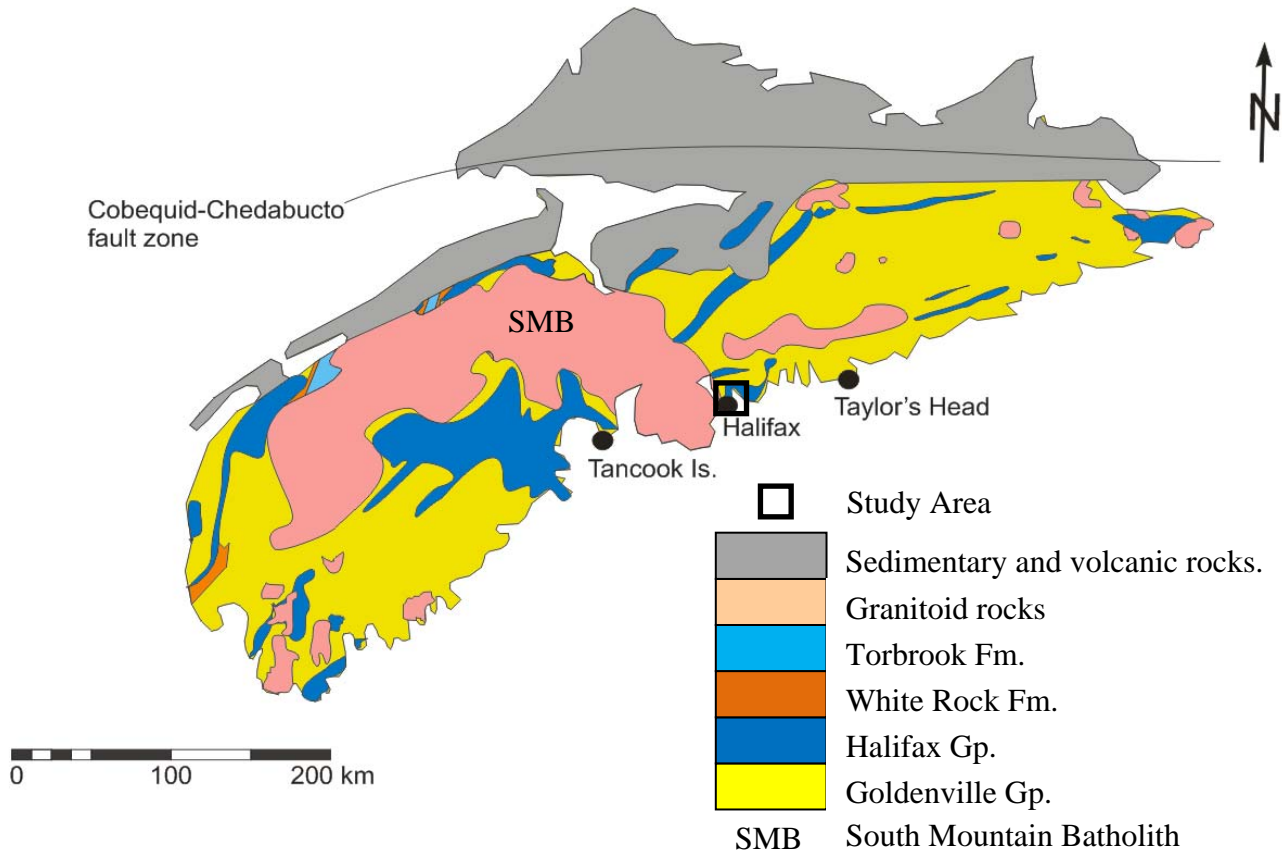
Figure 1.1 Distribution of the Palaeozoic groups and formations in Nova Scotia (Modified from Waldron et al., 2009).

The Halifax Group overlies and intertongues with the sediments from the Goldenville Group (Harris and Schenk, 1975), and both groups make up the Meguma

2

Supergroup. The Halifax Group (Fig. 1.2) is made up of the Mosher's Island,

Beaverbank, Cunard, Bluestone, Feltzen, Delanceys, and Rockville Notch formations

(Schenk, 1997; White et al., 2007). These formations were metamorphosed and folded in

the Devonian during the Acadian Orogeny (Harris and Schenk, 1975).

Figure 1.2: Stratigraphic column of the Meguma Supergroup. Adjacent formations are stratigraphically equivalent but are found in different locations (White et al. 2009; Schenk 1997)

In general, the Halifax Group is made up of meta-siltstone, slate, and a small

amount of meta-sandstone (Stow et al., 1984). The sandstones and siltstones comprise of

quartz and feldspar, with minor amounts of epidote, apatite, tourmaline, zircon, ilmenite,

and micas. The low grade metamorphosed rocks contain chlorite, muscovite, biotite, and

sericite (Stow et al., 1984). The provenance of the sediments was from the south east

(Harris and Schenk, 1975). The sandy layers of these outcrops come from cratonic,

quartz-rich provenance (Schenk, 1970; Harris 1971), from peri-Gonwandan terranes located adjacent to West Africa (Waldron et al., 2009). Lithofacies and physical sedimentary structures in the group include laminations of silty to fine-grained sandstone, and silty-fine grained sandstone with climbing ripples (Stow 1984).

The Beaverbank Formation overlies the Taylors' Head Formation and is made up of grey to green-grey thin bedded to laminated meta-siltstone and black slate (White et al., 2007). The Beaverbank Formation was interpreted by Ryan et al. (1996) as a transitional interval between the top of the Goldenville Group and base of the Halifax Group. The manganese in the layers correlate with the Moshers Island Formation (White et al., 2007), providing an age range of the Beaverbank Formation from the mid to late Cambrian based on the fauna (Pratt and Waldron, 1991).

Overlying the Beaverbank Formation is the Lower Ordovician Cunard Formation, made up of slate, meta- siltstone, and cross-laminated meta-sandstone. The formation also contains disseminated sulphide minerals including pyrite, arsenopyrite, and pyrrhotite (White et al., 2007).

The outcrops found in Point Pleasant Park are part of the Bluestone Formation (Fig. 1.3) which overlies the Cunard Formation and is Lower Ordovician in age. The formation is very similar to the Cunard Formation, comprising laminated meta-siltstone and slates; with the addition of fine-grained meta-sandstone which is absent in the Cunard Formation and contains calcareous nodules, which also helps differentiate the Bluestone from the Cunard Formation. (White, 2007). The Bluestone is equivalent to the Feltzen Formation (White et al., 2007), and was considered by White (2009) to be up dip

stratigraphic equivalent to the Bluestone. The outcrops comprise laminated meta-siltstone

and fine-grained meta-sandstones.
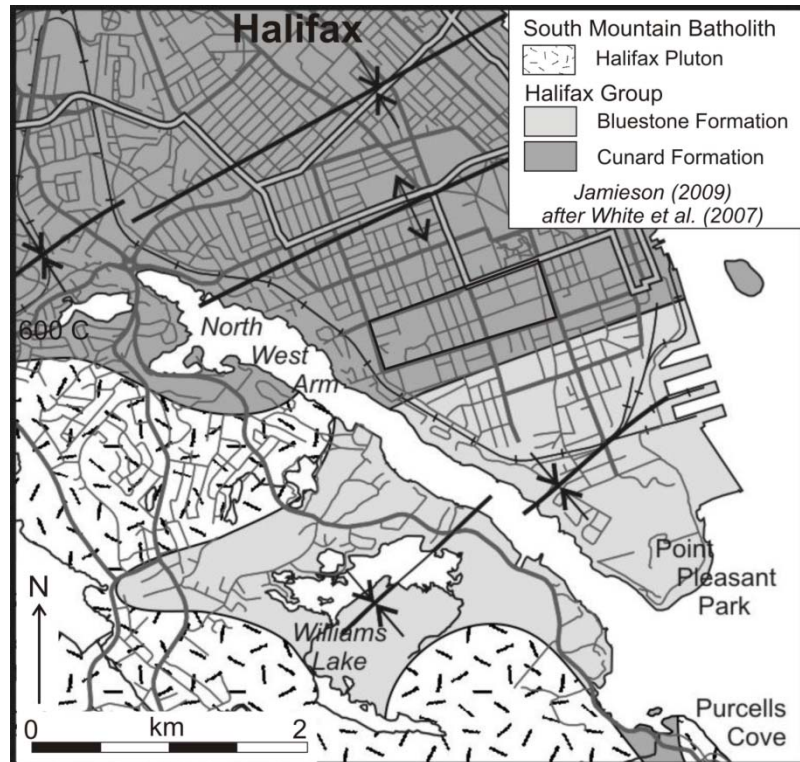
Figure 1.3: Geological map of Halifax showing the Cunard and Bluestone formations and the Halifax Pluton of the South Mountain Batholith (Jamieson 2009), after White et al., 2007).

1.4 Bouma Sequence

The Bouma sequence (Bouma, 1962) (Fig. 1.4) is a fining upward sequence of

five divisions characterized by grain size and sedimentary structures, deposited under

turbiditic flow. The five divisions of the Bouma sequence of a turbidite, begin at the base

with A-structureless sandstone, B-laminated sandstone, C-silty-sandstone climbing

ripples, D-siltstone lamina, and are capped with, E-structureless shale.
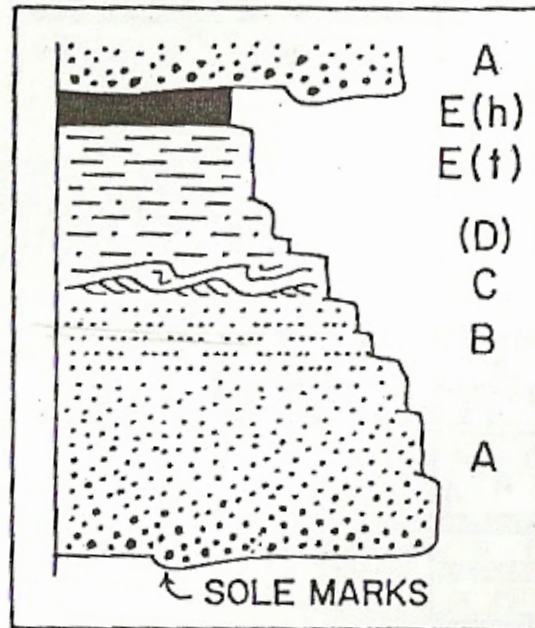
Figure 1.4: Diagram of the five divisions of the Bouma sequence showing the lithology, grain size, and sedimentary structures (Bouma, 1962).

This template will assist in the interpretation of the outcrop; recognizing that there are variations of the Bouma sequence depending on the calibro of the grain size inherent in the depositional system (Orton and Reading 1991) and the location of the 'sample' on the 'turbidite'.

1.5 Flow Processes

There are three different types of flow processes; homopycnal, hyperpyncal, and hypopycnal flows. Homopyncal flows are where the water is equal to the density of the standing water in the basin which causes rapid mixing through the flow (Walker and James, 1992). A Hypopycnal flow is where a lower water density enters denser standing water in the basin. The sediment is suspended in the flow until flocculation drops the suspended load through the denser water column into the basin (Walker and James, 1992). Hyperpyncal flow is until the water entering the basin is greater than the density

of the standing water in the basin. Mixing of the sediment happens on the side of the

flow and the moving sediments erode the sediments from the bed. These sediments are

what form turbidite deposits (Walker and James, 1992).

1.6 Coarse Grained Turbidite Model

      The coarse grained turbidite begins with a massive coarse grained sandstone

(R_1), followed by stratified (R_2), graded-stratified (S_1), and is often capped by dish and

pipe dewatering structures, the S_2 division of Lowe (1982). The coarse grained turbidite

model is mainly made up of medium to coarse grained sandstone (Lowe, 1982) (Fig. 1.5)
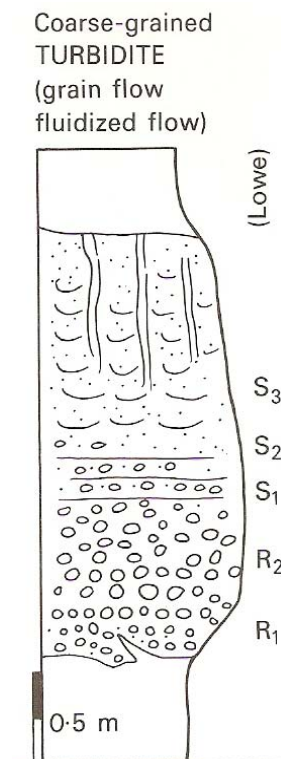
*Figure 1.5: Stratigraphic column of coarse-grained turbidites with the divisions
proposed by (Lowe, 1982).*

1.7 Fine-grained Turbidite Model

      For fine-grained turbidite models Piper (1978) proposed further divisions mainly

made up of the divisions D and E. The sub divisions are silt laminated mud (E_1), graded

mud (E_2), and non-graded mud (E_3) (Piper, 1978) (Fig. 1.6). Stow (1980) (Fig. 1.8)

recognized lenticular siltstone lamina with climbing ripples at the top (T_0), a thick mud

layer with convolute silt lamina (T_1), low amplitude ripples (T_2), parallel distinct (T_3),

parallel indistinct (T_4) and wispy silt laminae (T_5). Graded mud (T_6), and non-graded

mud (T_7) and a microbioturbated layer (T_8) to cap the succession (Stow and Shanmugan,

1980).
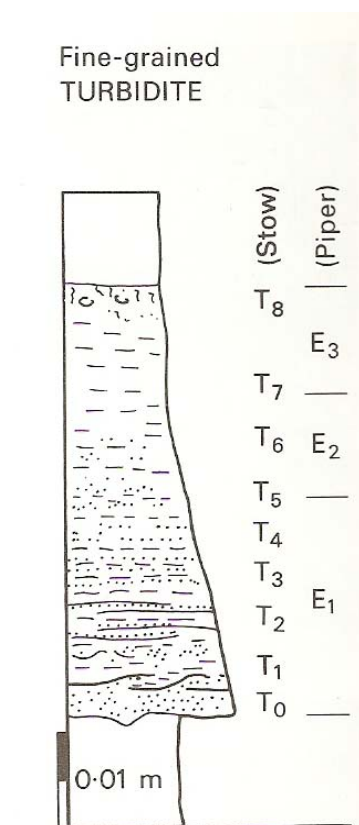
Figure 1.6: Comparison of the stratigraphic column of fine-grained turbidites with divisions determined by Stow (1980) and Piper (1978).

1.8 Fine-Grained Turbidites compared to Coarse Grained Turbidites

Fine-grained turbidites can be found on the distal areas of a coarse grained

turbidite flows, in the levee and overbank deposits adjacent to the submarine channels.

As the turbidite flows through the submarine channels, coarser material is deposited in

the channel while the finer grained sediments are deposited on the overbanks of the

channel (Fig. 1.7). As the sediments are deposited, they settle into the T_{c-d} divisions.

These sediments form the Bouma sequence as they settle out from suspension, depositing

fine-grain sand massive or sand current ripples, and sand to silt with parallel laminations

(Bouma, 2000; Kirschner and Bouma, 2000).

On the coastal plain, low gradient fluvial channels allow coarser sediment to

settle (Stelting et al., 2000).
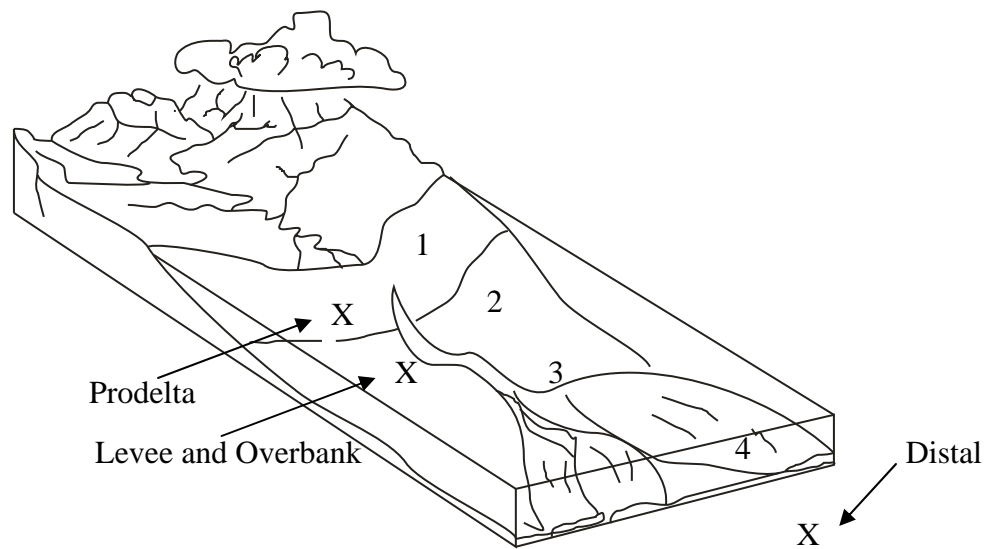
Figure 1.7: Diagram showing the stages of a fine-grained turbidite system (Modified from Stelting et al, 2000). Shown in the X are the possible locations of fine-grained turbidite deposition. The numbers represent the different steps described in the text.

As sea level drops, and accommodation space decreases, either a delta can

prograde across the shelf, or incision and bypass of sediment through a canyon can occur

(Fig. 1.7).

(**1**) (Bouma, 2000; Wach et al. 2000). As the sediment on the shelf aggrades, the

pore pressure may increase to a point where the sediment is unstable causing a flow

(Stelting et al., 2000). This can cause downslope mass transport and subsequent scouring

of the slope (**2**) (Wach et al., 2000; Bouma, 2000). As the gradient becomes less steep,

the sediment begins to deposit as a massive structureless sand (**3**) (Stelting et al., 2000). As the flow continues into the basin, the sediments become more sorted and sedimentary structures start to form (**4**) (Stelting et al., 2000). The sediments can also infill previously scoured and form levees with lamina and climbing ripples on the overbank deposits (**4**) (Stelting et al., 2000).

This fine grained, low density turbidity model is different from the coarse-grained turbidite model in several ways; the coarse grained turbidite model is typically more sand-rich due to proximity to source, and possibly the lack of a delta trapping sediment, in the case of deepwater fans linked to canyons. These turbidites are found proximal to their source such as a delta front, the toe slope, or in submarine channels while the finer grained material is found on overbanks, levees, or distal from the source. Coarse sediment can be mobilized as longshore drift deposited along the shore, away from the entry point. Shorelines can prograde and gradually infill the canyon head (Stelting et al., 2000). Similar to fine-grained turbidites, the aggraded sediment can become unstable and move down the canyon allowing the slope or basin floor fan to prograde basinward (Stelting et al., 2000).

A turbidite can be completely fine grained if the source of the sediment is fine grained. This is evident from turbidites that have been sourced from the Mississippian and Rhone deltas (Orton and Reading, 1991).

1.9 High and Low Density Turbidites

High-density turbidites is the body of the turbidite that deposits in submarine channels and proximal fan. Low-density turbidites is the sediment that is deposited on the overbanks and levees, and the distal section of the fan.

2. <u>Methodology</u>

2.1 Field Overview

Previously mapped outcrops from Tobey's (2004) study were used to locate outcrops for this study. The development of new pathways in the park in 2005, exposed new outcrops in the dense vegetation and these were recorded on the map. Of the 21 that Tobey (2004) recorded, 10 outcrops were selected for examination in this study based on the presence and clarity of the sedimentary structures such as Black Rock Beach and Sailors' Memorial Rd.

2.2 Outcrop Logging

The outcrops (Fig. 3.1) were examined in great detail. Each outcrop was logged recording grain size, thickness and physical and biogenic sedimentary structures (if present). After the logs were completed, they were digitally processed into the ALT Well Cad and Core Cad software for analysis.

2.3 LiDAR (refer to Appendix II)

Optech ILRIS LiDAR (Fig. 2.1) is an optical remote sensing technology with application such diverse studies as architecture to coastal mapping. It measures the time between laser impulses and laser detection. LiDAR was used to produce 3D images of the outcrops for detailed photogrammetric analysis. The detailed images can be used for constructing geologic models and modeling reservoir potential. The LiDAR is positioned 2-4m in front of the outcrop and scans the face. The LiDAR measures the time delay between laser pulses and the reflection signal from short wavelengths similar to UV light and infra-red waves. The LiDAR is able to discern with high resolution physical sedimentary structures, changes in lithology, and penetrate the surface outcrops

that are covered in lichens and vegetation to a degree not recognized prior to this study. LiDAR imaging has an advantage over taking a picture because the scans provide increased detail. The point cloud data was put into Petrel and Polyworks to analyse structures, bedforms and architectural elements that were not readily apparent before analysis of the processed LiDAR data. Limitation to this technique is knowing the distance that is needed for optimal scanning potential. If the LiDAR is close to the outcrop and the surface of the outcrop is very smooth, there is the potential of long scanning times, and the laser bouncing off the outcrop at spurious angles and not reflecting back to the LiDAR. The drain on the batteries used for the LiDAR limit the number of images scanned in one day, so careful scan planning needs to be done to optimize field time.

Figure 2.1: Photo of the Optech ILRIS LiDAR.

2.4 AUSlog Scintillometer Analysis (Also refer to Appendix I)

Certain clastic sediment will give off more gamma ray particles than others.
Shales and shaly rocks contain more thorium, uranium, and potassium than sandstones
bound to clay minerals like kaolinite and smectite that contain more reactive minerals
giving higher GR values. The AUSlog scintillometer (Fig. 2.2) measures the amount of
gamma ray particles that are emitted from the rock. If there are less of these minerals in
quartz rich sandstone the gamma ray reading will be low. The results can be plotted to
demonstrate a gamma ray well log signature. This can be used to help correlate the
outcrops and differentiate lithology and depositional cycles. The advantages of using the
AUSlog is the data is sent and recorded onto a hand held computer (PDA). The PDA can
send the data to the computer and rapidly plotted. The API scales used for plotting the
scintillometer data is 0-150, the standard scale used in oil and gas logging.

AUSlog Scintillometer

Hand Held Computer

Figure 2.2: Photo of the AUSlog scintillometer.

2.5 Petrographic Analysis

Thin sections were made from samples from outcrops to determine representative lithologic composition, and relationships between colour change, grain size, and sedimentary structure.

2.6 Paleocurrent Analysis

Paleocurrents were measured by recording the orientation of the climbing ripples and tool marks from the surfaces of the outcrop. Climbing ripples on the top and side of the outcrop were checked to make sure that ripples were not boudinage structures formed during low grade metamorphism. The Meguma Supergroup has been deformed so a stereonet was used to unfold the structure and place the ripples and tool marks into the correct orientation. Ripple and tool mark orientations were then placed on a Rose diagram so that the primary orientation of the paleocurrent could be determined.

3. <u>Results</u>
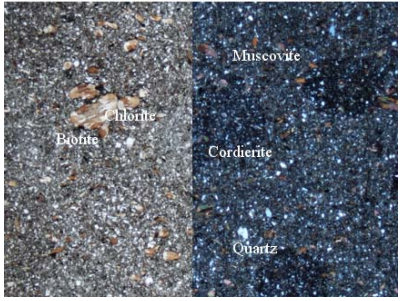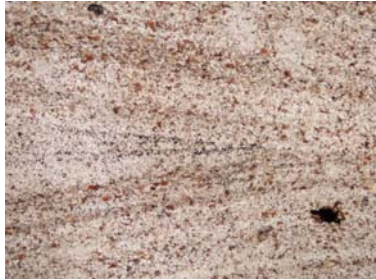
3.1 Introduction

        The data results described in this chapter are provided by the measured sections, LiDAR, scintillometer, petrographic, and paleocurrent analysis. The results determine the lithology, mineral composition, and sedimentary structures so that lithofacies assemblages can be discerned. These will be used to correlate the outcrops, determine the paleocurrent orientation and direction of initial sediment transport. Metamorphic grade will be examined. The outcrops have experienced low grade metamorphism and effects of the metamorphism on the strata and the sedimentological interpretation were recorded from petrographic analysis and observations of the measured sections.

3.2 Lithofacies and Lithofacies Association

        The outcrops comprise lithofacies of structureless meta fine-grained sandstone, meta silty-sandstone laminae, meta sandy-siltstone climbing ripples, meta-siltstone laminae, and a structureless silty slate to slate (Table 1) which make up a turbiditic lithofacies association.

Table 1: Lithofacies characteristics with outcrop scale and representative thin section images.

Lithofacies Description	Outcrop Image	Thin Section
Structureless silty slate to slate 5-10cm thick, Rich in mica and cordierite Reference thin section: PPP04-15		

Laminated siltstone
Max 2cm thick laminae,
max 40cm thick laminae sets, rich in mica and cordierite but more quartz present, quartz is very fine grained
Reference thin section:
  PPP04-06
  PPP04-09
  PPP04-30		

Climbing rippled sandy-siltstone
Climbing Ripples 1-5cm amplitude, 5-50cm thick, quartz and mica is equal, quartz very fine grained
Reference thin section:
  PPP04-05b
  PPP04-06
  PPP04-30		

Laminated silty-sandstone
Max 2cm thick laminae,
max 40cm thick laminae sets, more quartz than mica, quartz is fine grained
  PPP04-03
  PPP04-05a		

Structureless meta sandstone 5cm-1m thick, quartz rich		

3.3 Measured Sections
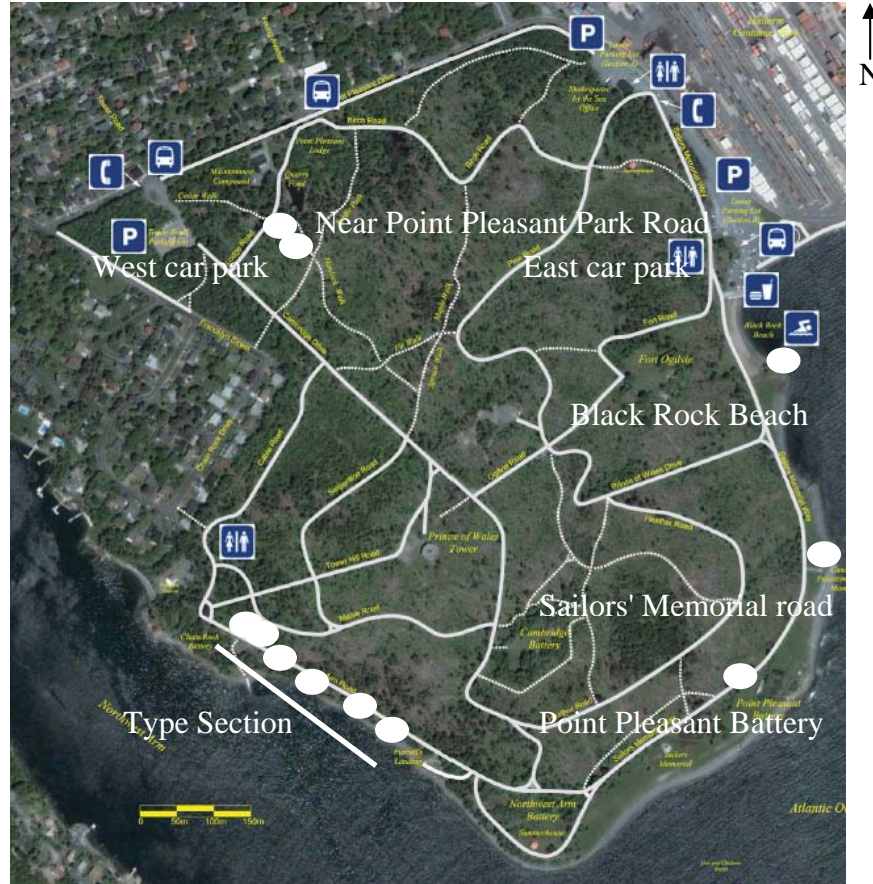
Figure 3.1: Satellite image of Point Pleasant Park showing the locations (black ovals are the outcrops used in the study). The outcrops are represented in the black circles (Image from Point Pleasant Park, 2008).

3.3.1 Sedimentological Type Section

The Sedimentological Type Section (Fig. 3.2) comprises four outcrops located

along the shore of the North West Arm of the park (Fig. 3.1). The measured section is

48.5 m in length and has a maximum width of 5 m. The dry colour ranges from medium

grey to black. Bedding has a structural dip 30° towards the north west.

Lithology ranges from fine-grained meta-sandstone to slate. Sedimentary

structures include climbing ripples and parallel laminae. The laminae and bed contacts

between the lithologies are gradual and sharp. The lithofacies show characteristics of the Bouma Sequence (Table 2). The outcrop is metamorphosed at a low grade, and contains holes where cordierite formed and later weathered out.

Structureless meta fine-grained sandstone lithofacies have a maximum thickness of 1 m, the laminated meta-silty sandstone lithofacies have a maximum thickness of 40 cm. The climbing rippled meta sandy-siltstone lithofacies have a maximum thickness of 50 cm. The laminated meta-siltstone lithofacies has a maximum laminae set thickness of 10 cm. The structureless slate to slate lithofacies has a maximum bed thickness of 20 cm. The measured section has beds of structureless meta fine-grained sandstone and laminated meta-siltstone lithofacies throughout the section. These lithofacies are between 1-1.5 m, 35.2-35.5m, 36.5-37.7 and 43.2-44.4m. There is a bed of thick structureless meta fine-grained sandstone at 43.2-44.4m. The meta siltstone lithofacies is found in the Sedimentological Type Section, in association with laminated meta silty sandstone and structureless slate lithofacies, or in combination with the climbing rippled meta sandy siltstone and structureless slate lithofacies (Table 2). The difference between the laminated meta silty sandstone and the laminated meta siltstone lithofacies is visible by a distinct change in colour within the laminae from brown sand to grey silt.

There are thick combinations of either climbing rippled meta- silty-sandstone and slate between 40.2-40.5m, laminated meta sandstone and slate such as between 40.5-42.2m, or laminated meta siltstone and climbing rippled meta silty-sandstone between 46.5-48.8m (Table 2). These thick combinations range between 0.5-1m and usually occur just before an interval of structureless fine-grained meta sandstone or laminated meta-silty in the sandstone. These combinations of lithofacies are related to variations of

18

the Bouma sequence (Table 2). The Sedimentological Type Section contains all five

lithofacies, but in general the section is made up of the three finer grained lithofacies:

climbing rippled meta sandy-siltstone, laminated meta-siltstone, and a silty slate to slate

structureless lithofacies (Table 2). The bed length of these lithofacies ranges from 5cm-

20cm but are mainly 10cm in thickness.

The lithofacies show a variety of length to thickness ratios (Table 3). The length

range is 10-17 m with the length of these beds become longer towards the top of the

outcrop. The length of these beds depended on the condition and exposure of the

outcrop. The thickness ranged from 0.02-1m with the laminated meta siltstone being

showing the smallest variation and thinnest thickness. The structureless fine grained

meta sandstone is the thickest, up to as 1m in thickness.

(a)

Sedimentological Type Section
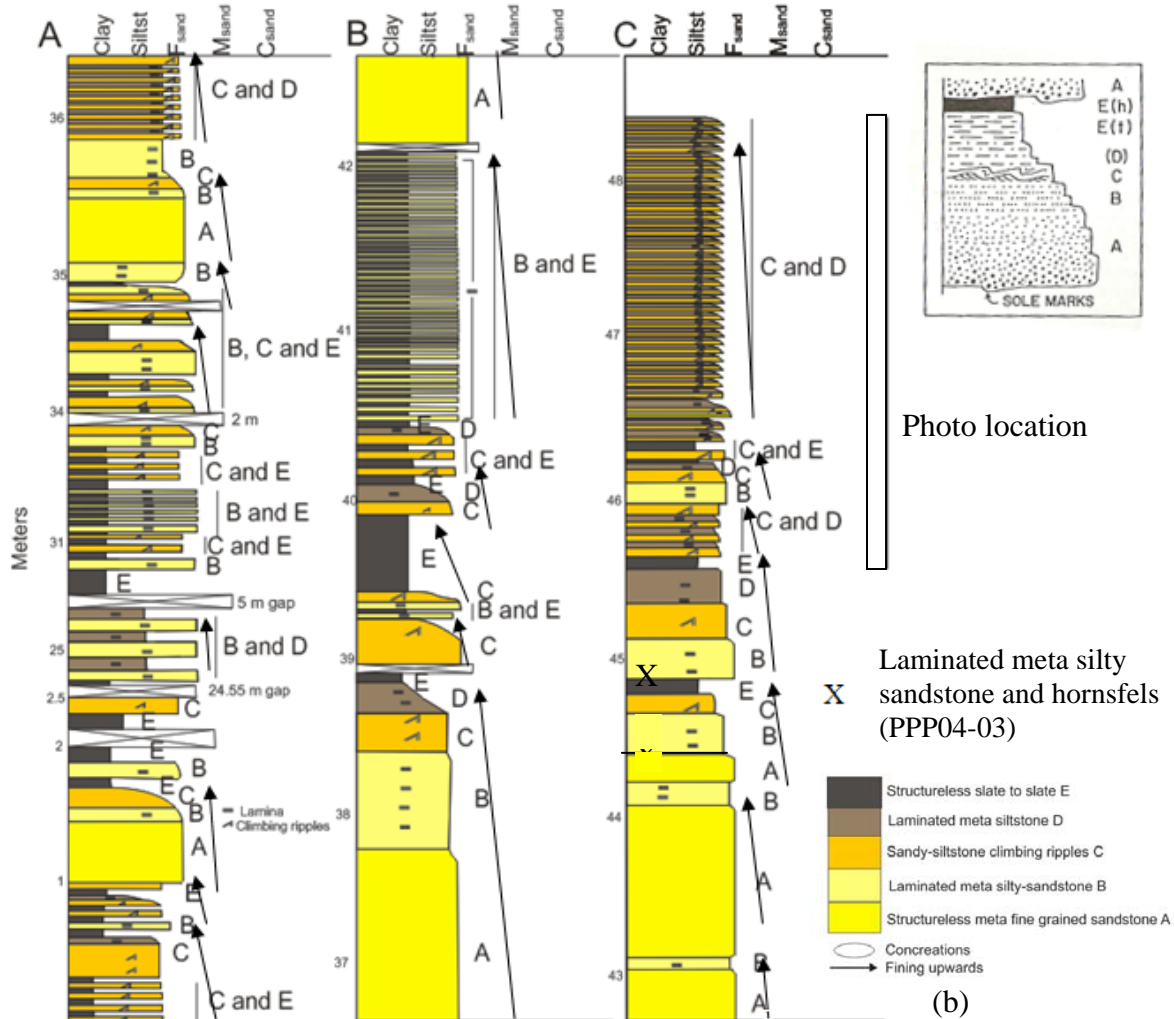
Figure 3.2: Annotated photo (a) and measured section of the Type Section (b). The lithology ranges from fine grained meta-sandstone to slate, and contains physical sedimentary structures like climbing ripples and parallel lamina. A the base of the measured section there are intervals of 1.0m thick massive meta sandstone beds followed by 30 cm thick beds of laminated meta sandstone and climbing rippled meta silty sandstone. This segment finishes with laminated meta siltstone and slate. The bedding and laminae sets become thinner, and certain lithofacies become more frequent such as laminated meta silty-sandstone, climbing rippled meta sandy-siltstone, and laminated meta-siltstone lithofacies between 46-46.4 m, and towards the top of the measured section (46.5-48.8m) meta silty-sandstone lamina and meta-siltstone lamina lithofacies dominate. Note gaps in the section at 2.5m, 25.5m, 32m, 38.9, and 42.2m.

Table 2: Combination of lithofacies relating to the divisions of the Bouma Sequence of the Type Section.

Bouma Division					
E	Structureless silty slate to slate			Structureless silty slate to slate	
D	Laminated meta-siltstone laminae	Meta-siltstone laminae	Meta-siltstone laminae		
C	Climbing rippled Meta sandy-siltstone	Meta sandy-siltstone climbing ripples		Meta sandy-siltstone climbing ripples	
B	Laminated Meta silty-sandstone	Meta silty-sandstone laminae	Meta sandy-siltstone climbing ripples		Laminated meta-silty sandstone
A	Structureless meta sandstone	Structureless meta sandstone			Structureless meta sandstone

Table 3: Length and thickness ratios of the lithofacies in the Type Section measured from different beds.

Bouma Division	Type Section	T (m)	L (m)	T (m)	L (m)	T (m)	L (m)	T (m)	L (m)
E	Structureless silty slate to slate	0.3	17.0	0.2	17.0	0.04	14.5	0.03	14.5
D	Laminated Meta-siltstone	0.1	17.0	0.05	10.0	0.03	14.0		
C	Climbing rippled meta sandy-siltstone	0.25	14.0	0.2	14.0	0.1	14.5	0.03	17.0
B	Laminated Meta silty-sandstone	0.4	14.0	0.25	14.0	0.1	14.5	0.05	14.0
A	Structureless meta sandstone	1	14.0	0.5	14.0	0.2	14.0	0.05	17.0

3.3.2 Black Rock Beach Measured Section

This outcrop is located on the sandy beach near the east car park of Point Pleasant Park (Fig. 3.1). The top of the outcrop is smooth and shows glacial striations. The outcrop is 2.5 m in height and 10 m in length, showed a dry colour change from grey to light grey, and the bedding is dipping 20° towards the north. GPS co-ordinates are 455295E 4941325N.

The lithology of the outcrop ranges between fine-grained meta sandstone to slate, with slate more common towards the top of the section. The sedimentary structures seen in the outcrop are thin laminations 1 mm, climbing ripple sets ranging 1-5 cm in amplitude, starved ripples 1 cm in amplitude, and structureless sediments. Starved current ripples are created by a lack of sand so the ripple cannibalizes ripples on the stoss side and deposits on the lee side. The ripples have an apparent higher angle of repose than the normal maximum of 30°, measured up to 60°. This is an effect of the tectonic shortening and metamorphism of the formation. Metamorphism also formed boudinage structures, which appear as pseudo climbing ripples. The massive beds are mainly made up of slate. Also found in the outcrop are carbonate concretions and carbonate or calcite layers. Minerals seen within these concretions include calcite identified from hydrochloric acid reactions. The concretions are oval shaped, 30cm in length and 10 cm thick with a reddish colour, which is different from the surrounding outcrop. There is also a folded calcite layer 5 cm thick and a 100 cm in length. The contacts are gradual where there is a sedimentary change,such as from laminae to climbing ripples reflecting a decrease in flow velocity, and sharp when there is a grain-size change such as from laminated meta silty sandstone to silty slate or slate.

The outcrop (Fig. 3.3) lithofacies comprise laminated meta silty-sandstone, climbing rippled meta sandy-siltstone, laminated meta-siltstone, and structureless meta siltstone lithofacies (Table 4). The thicknesses of the lithofacies vary; laminated meta silty-sandstone, climbing rippled meta sandy-siltstone, and laminated meta-siltstone lithofacies have a thickness range of 2-6 cm, while the slate lithofacies have a thickness range of 1-10 cm (Table 5). The lithofacies in this outcrop tend to thicken and thin throughout the outcrop, however generally the bed thicknesses are becoming thinner towards the top between 1.65-2.2m. Laminated mta silty-sandstone, climbing rippled meta sandy-siltstone climbing ripples, and structureless silty slate to slate lithofacies are between 0-1.65m of the outcrop but the top the interval occasionally has meta-siltstone laminae lithofacies. 1.65-2.2m, climbing rippled meta sandy-siltstone and laminated meta-siltstone lithofacies dominate. These combinations range 5-20cm in thickness.

The lengths of the parallel beds are 15 m. The outcrop was eroded so the length would have extended further (Table 5). The thicknesses of the lithofacies do not show a large variation as the range is 3-15cm with most of the beds being 10 cm.

Table 4: Combination of lithofacies relating to the divisions of the Bouma Sequence at Black Rock Beach.

Bouma Divisions			
E		Silty slate to slate	Silty slate to slate
D	Laminated meta-siltstone		
C	Climbing rippled meta sandy-siltstone	Climbing rippled meta sandy-siltstone	Climbing rippled meta sandy-siltstone
B	Laminated meta silty-sandstone	Laminated meta silty-sandstone	
A			

Table 5: Length and thickness ratios of the lithofacies at Black Rock Beach

Bouma Divisions	Black Rock beach	T (m)	L (m)	T (m)	L (m)
E	Structureless silty slate to slate	0.15	15.0	0.15	15.0
D	Laminated mta-siltstone	0.10	15.0	0.05	15.0
C	Climbing rippled Meta sandy-siltstone	0.03	15.0	0.10	15.0
B	Laminated meta silty-sandstone	0.10	15.0	0.03	15.0
A	Structureless meta sandstone				

Black Rock Beach
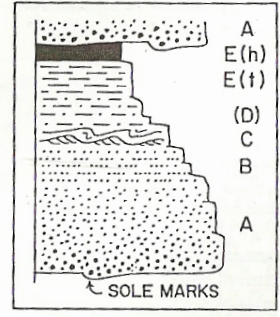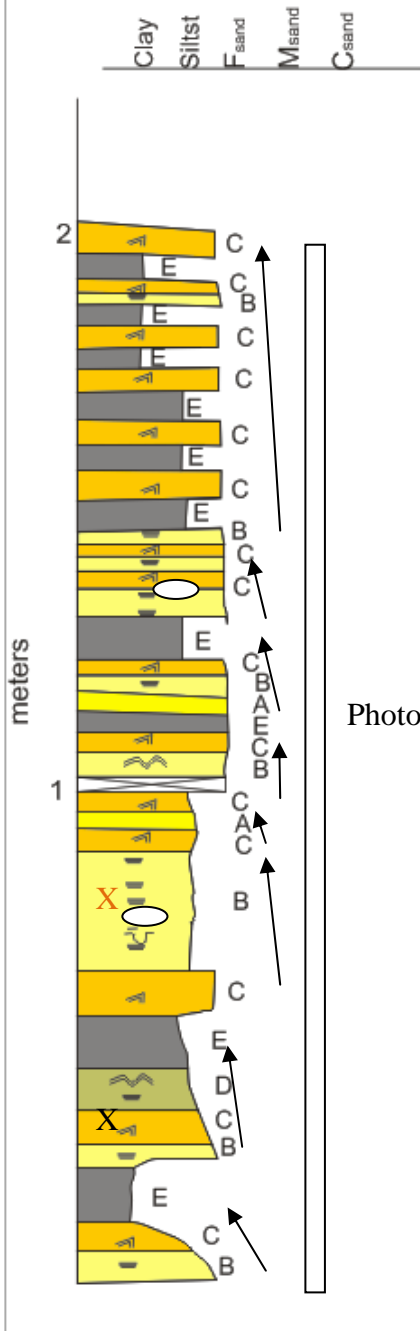
X Climbing rippled Meta
   sandy-siltstone and meta
   siltstone (PPP04-30)

X Laminated meta silty
   sandstone (PPP04-09)

Structureless slate to slate E

Laminated meta siltstone D

Sandy-siltstone climbing ripples C

Laminated meta silty-sandstone B

Structureless meta fine grained sandstone A

◯ Concreations

→ Fining upwards

≡ Laminae
⊿ Climbing ripples
∿ Wavy laminae
⌄ Load Structures
Ξ Parallel Bedding

(a)

(b)

Figure 3.3:Measured section of Black Rock Beach outcrop (a) and an annotated photo of the outcrop (b). The lithology ranges from fine-grained meta-sandstone to slate, and contains sedimentary structures like climbing ripples and parallel laminae. This measured section consists of laminated meta silty-sandstone, climbing rippled meta sandy-siltstone, laminated meta-siltstone, and a structureless silty slate to slate lithofacies with climbing rippled meta sandy-siltstone, laminated meta-siltstone, and a silty slate to slate lithofacies more common towards the top of the measured section. Also the laminae set thicknesses become thinner towards the top with the 20 cm last bed starting a new cycle of thick beds.

3.3.3 Point Pleasant Battery

There are two outcrops found around the Battery. One is in front of the Battery and one behind. This outcrop measured is behind the Battery (Fig. 3.1). The outcrop is 2 m in height and 15 m in length, and dry colour varies vertically from light to dark grey. The bedding is dipping 20° towards the north west. The GPS co ordinates are 0455241E 4940944N.

This outcrop (Fig. 3.4) is made up of fine-grained meta-sandstone to meta siltstone. The sedimentary structures found in this outcrop are laminae 1 mm in thickness, and climbing ripples range from 5- 10 cm long. The bedding in this outcrop ranges from 10 cm to 50 cm thick. The outcrop is moderately metamorphosed evident from the holes where cordierite was formed, and weathered out and slate. One calcite concretion is found in the upper middle interval of the outcrop. The concretion is 10cm thick and 1 m in length. The inside of the concretion is red and pinkish red on the outside, due to exchange of elements likely iron oxides.

This outcrop is made up of two major cycles (Table 6) made up of laminated meta silty-sandstone laminae, climbing rippled meta sandy-siltstone, laminated meta-siltstone, and a structureless silty slate to slate lithofacies, and are related to the Bouma sequence. The cycles are similar in thickness between 0.6-0.7m and the lithofacies change gradually in this outcrop. The laminated meta silty-sandstone are 10-30 cm thick, the climbing rippled meta sandy-siltstone are 5-20 cm thick, the laminated meta-siltstone lithofacies is 30-40 cm thick, and structureless slate lithofacies is 10 cm thick (Table 7).

The bed length of these lithofacies ranges 7.2-14.4m (Table 7). Lithofacies showed lateral continuation across the outcrop until truncated where the beds entered the hill side.

Table 6: Combination of lithofacies relating to the divisions of the Bouma Sequence at Point Pleasant Battery.

Bouma Division		
E	Structureless silty slate to slate	
D	Laminated meta-siltstone	Laminated meta-siltstone
C	Climbing rippled meta sandy-siltstone	Climbing rippled meta sandy-siltstone
B	Laminated meta silty-sandstone	Laminated meta silty-sandstone
A		

Table 7: Length and thickness ratios of the lithofacies at Point Pleasant Battery measured from different beds.

Bouma Division	Battery	T (m)	L(m)	T (m)	L (m)	T (m)	L(m)
E	Structureless silty slate to slate	0.1	7.2				
D	Laminated meta-siltstone	0.3	14.4	0.1	7.2		
C	Climbing rippled meta sandy-siltstone	0.23	7.2	0.05	7.2	0.03	14.4
B	Laminated meta silty-sandstone	0.1	7.2	0.3	14.4		
A	Structureless meta sandstone						

Point Pleasant Battery
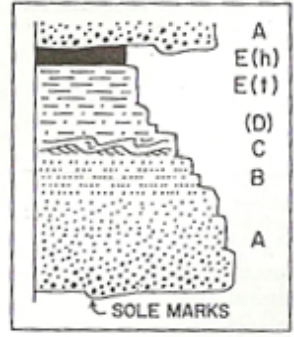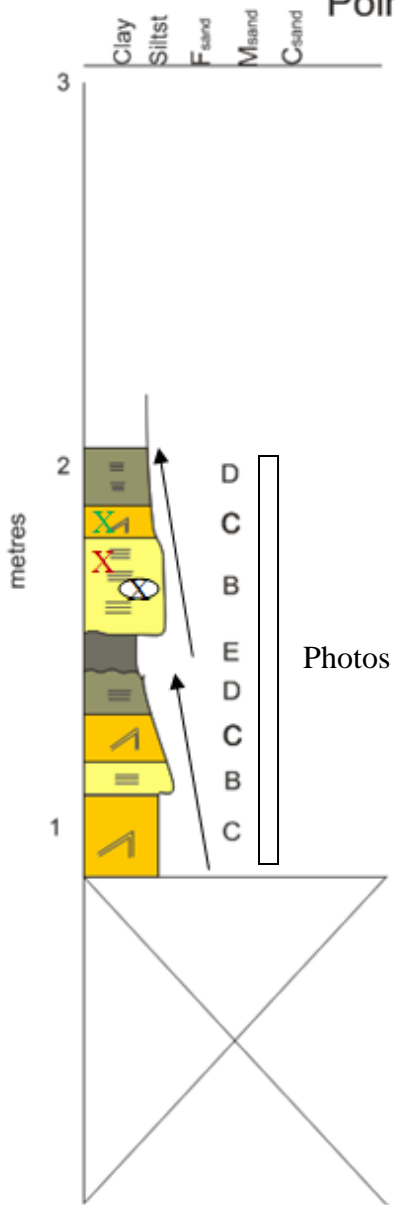
X   Concretion (PPP04-05)
X   Laminated meta silty sandstone (PPP04-05a)
X   Climbing rippled meta sandy-siltsone (ppp04-05b)

Photos

⬛	Structureless slate to slate E
⬛	Laminated meta siltstone D
🟧	Sandy-siltstone climbing ripples C
🟨	Laminated meta silty-sandstone B
🟨	Structureless meta fine grained sandstone A
⬭	Concreations
→	Fining upwards

≡ Laminae
⟋ Climbing ripples
〜 Scoured
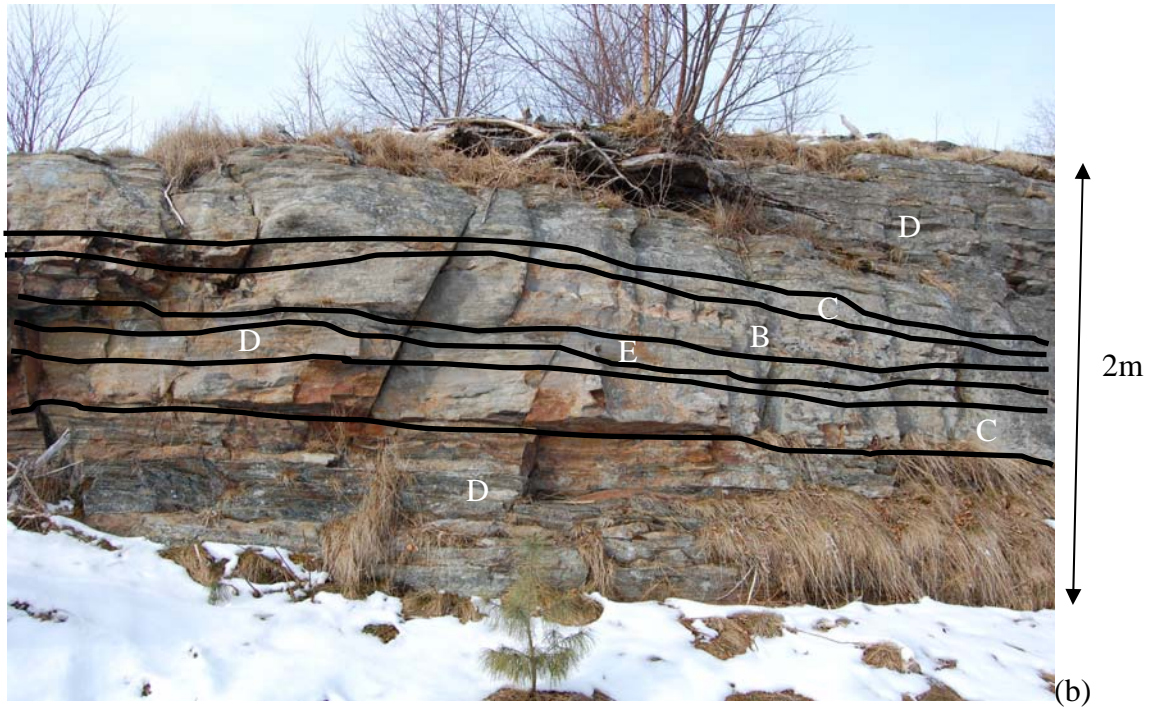
(a)

29

Figure 3.4: Measured section of the outcrop behind Point Pleasant Battery(a) and photo of the outcrop (b). The lithology ranges from fine-grained meta sandstone to slate, and contains sedimentary structures including climbing ripples and laminae. This measured section contains thick bedding of laminated meta silty-sandstone laminae, climbing rippled meta sandy siltstone, laminated meta-siltstone, and a structureless silty slate to slate lithofacies. The bedding thickness changes very little in the outcrop, but does thin around 1.6 m.

3.3.4 Sailors' Memorial Road

This outcrop is located on the rock beach next to the Sailors' Memorial Road (Fig. 3.1), and is just over 3 m in height and 5 m in length (Fig. 3.5). The dry colour ranges from brown to black, and the bedding dips 26° towards the north west.

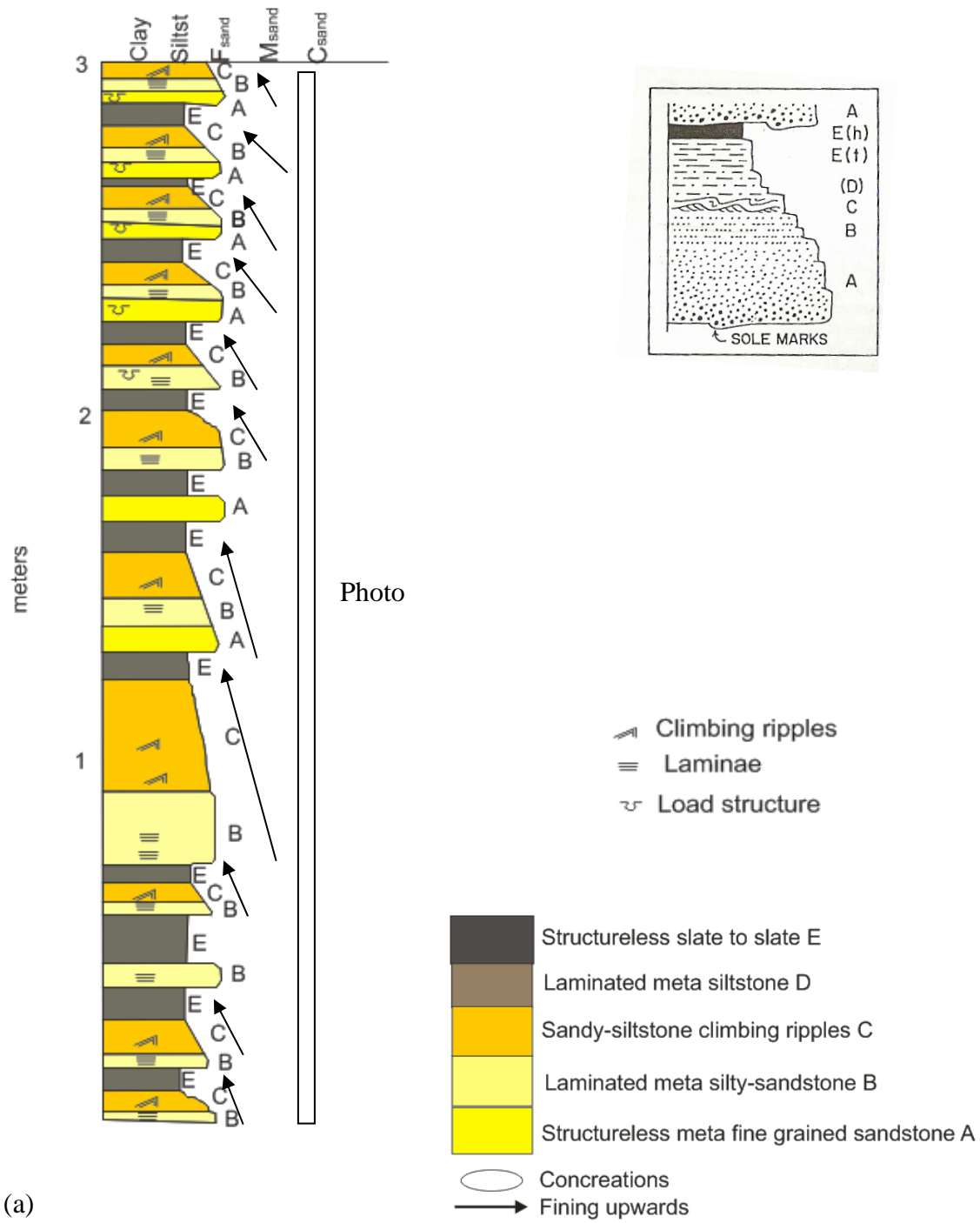The lithology is fine-grained meta-sandstone to slate with slate found at the top of the measured section. The sedimentary structures found included thin bedded laminae 1 mm thick, and climbing ripple sets 5 cm high. The contacts between lithologies range from gradual, sharp to scoured contacts. The bed thickness of the beds thin towards the top. The bed thickness ranged from 10-20 cm. No concretions were noted in this outcrop.

The outcrop shows evidence low grade metamorphism due to the holes where cordierite was formed and weathered and the formation of slate.
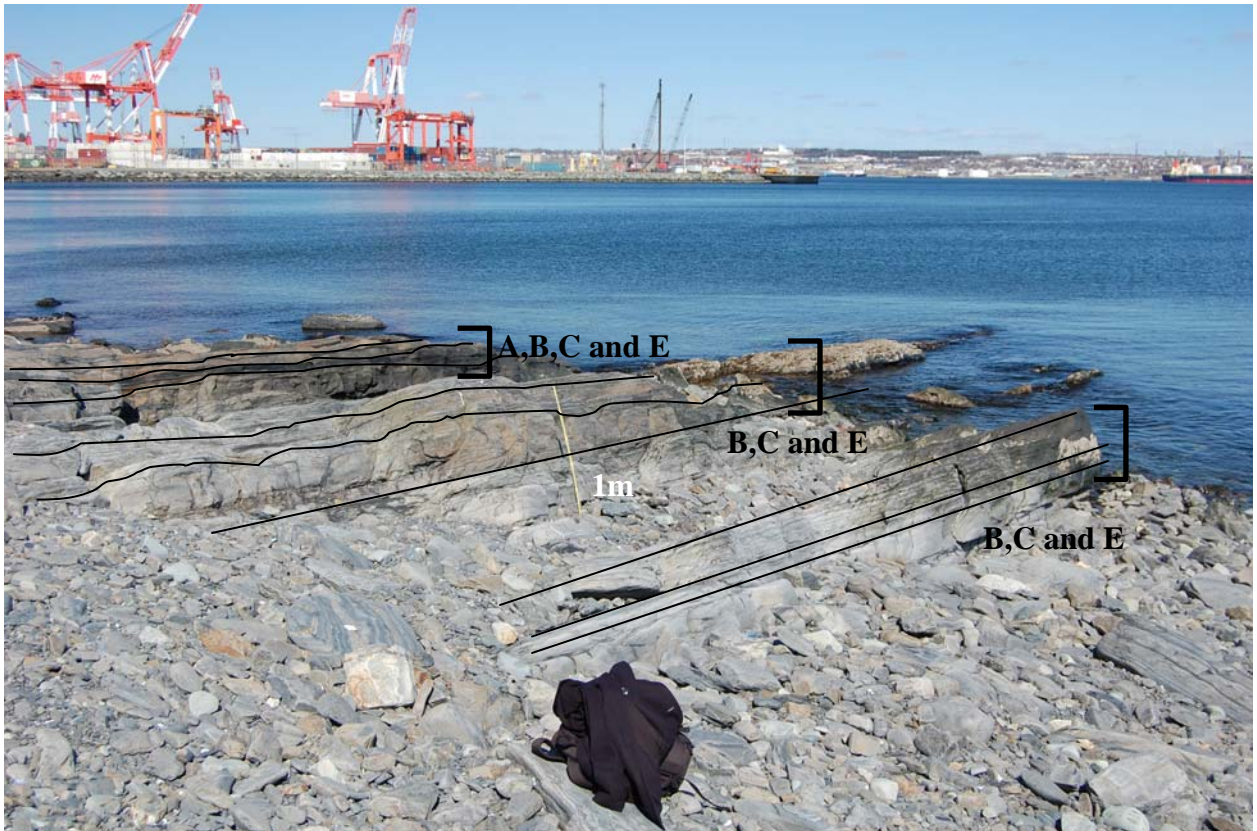
The outcrop shows structureless meta fine-grained sandstone, laminated meta silty-sandstone, climbing rippled meta sandy-siltstone, laminated meta-siltstone, and a structureless silty slate to slate lithofacies (Fig. 3.5a and Table 8). The structureless meta fine-grained sandstone, laminated meta silty-sandstone, laminated meta-siltstone, and a structureless silty slate to slate lithofacies have a maximum thickness of 5 cm, and meta sandy-siltstone climbing ripples have a maximum bed thickness of 20 cm and show characteristics of the Bouma sequence (Table 8 and 9, and Fig. 3.5a). From 0-1.5 m, the measured section shows sharp changes in lithofacies and only three lithofacies are present. The interval is dominated by laminated meta silty-sandstone and structureless silty slate to slate lithofacies. Climbing rippled meta sandy-siltstone and laminated meta-siltstone lithofacies appear occasionally. From 1.5 to 3.2 m, structureless meta fine-grained sandstone, climbing rippled meta sandy-siltstone, and structureless silty slate to slate lithofacies dominate, separated by a scoured contact. These lithofacies repeat throughout this portion of the outcrop. Also in this interval of the measured section, the structureless silty slate to slate lithofacies increases to slate towards the top. The cycles range 20cm-30 cm in thickness.

The lithofacies have a maximum length of 24m (Table 9). The lithofacies that show the least amount of variation was the meta siltstone laminae where the thickness was consistent across the outcrop.

Sailors' Memorial Road

(a)

Climbing ripples
Laminae
Load structure

Structureless slate to slate E
Laminated meta siltstone D
Sandy-siltstone climbing ripples C
Laminated meta silty-sandstone B
Structureless meta fine grained sandstone A
Concreations
Fining upwards

(b)

Figure 3.5: Measured section at Sailors' Memorial Road (a) and annotated photo (b). The lithology ranges from fine-grained meta-sandstone to slate, and contains sedimentary structures like climbing ripples and parallel laminae. This measured section contains structureless meta fine-grained sandstone ,laminated meta silty-sandstone, climbing rippled meta sandy-siltstone, laminated meta-siltstone, and a structureless silty slate to slate lithofacies, but the structureless meta fine-grained sandstone lithofacies is present between 1.6- 3.2 m, while absent between 0-1.6 m. The lithofacies generally do not change gradually from 0-1.6 m, however the lithofacies becomes gradual between 1.6-3.2 m.

Table 8: Combination of lithofacies relating to the divisions of the Bouma Sequence at Sailors' Memorial Road.

Bouma Division				
E	Structureless silty slate to slate	Structureless silty slate to slate	Structureless silty slate to slate	
D	Laminated meta silty-sandstone			Laminated meta silty-sandstone
C	Climbing ripples meta sandy-siltstone	Climbing ripples meta sandy-siltstone	Climbing ripples meta sandy-siltstone	
B		Laminated meta silty-sandstone		Laminated meta silty-sandstone
A	Structureless meta sandstone			

Table 9: Different length and thickness ratios of the lithofacies in Sailors' Memorial Rd measured from different beds.

Bouma Division	Sailors' Memorial Rd	T (m)	L (m)	T (m)	L (m)	T (m)
E	Structureless silty slate to slate	0.03	24.0	0.1	24.0	
D	Laminated meta silty-sandstone	0.05	24.0			
C	Climbing ripples meta sandy-siltstone	0.2	24.0	0.1	24.0	0.05
B	Laminated meta silty-sandstone	0.03	24.0	0.1	24.0	
A	Structureless meta sandstone	0.05	24.0	0.02	24.0	

3.3.5 Composite measured section

After analyzing the measured sections in detail and their distribution throughout the park, it became apparent that they represented a relatively continuous section of the Bluestone Formation from south east to north west. They were placed on top of each other in stratigraphic hierarchy (refer to Appendix III). The individual sections combined

length of the measured sections were added, recognizing that these outcrops have been folded and deformed and are on the limb of a syncline.

There are seven major cycles visible on the log. These cycles range from 1m-5.3m and start with the thick structureless fine-grained sandstone beds to thin structureless silt slate to slate beds. Within these major cycles are series of smaller fining upward cycles. The base of the cycles begin with coarser-grained lithofacies and finer-grained lithofacies mark the top of these major cycles.

The true thickness composite log (refer to Appendix IV for a large size) is 242m comprising the measured sections and the missing section of outcrop. The gaps range from 2m-100m. These are likely thick intervals of slate that have preferentially been eroded away due to their fissile nature. Evidence of these intervals of slate is found on Francklyn St. and on Point Pleasant Park Drive. Rare sedimentary structures, such as starved current ripples are seen in these outcrops, but are absent in the park itself.

Structureless silty slate to slate
Laminated meta siltstone
Climbing rippled meta sandy-siltstone
Laminated meta silty-sandstone
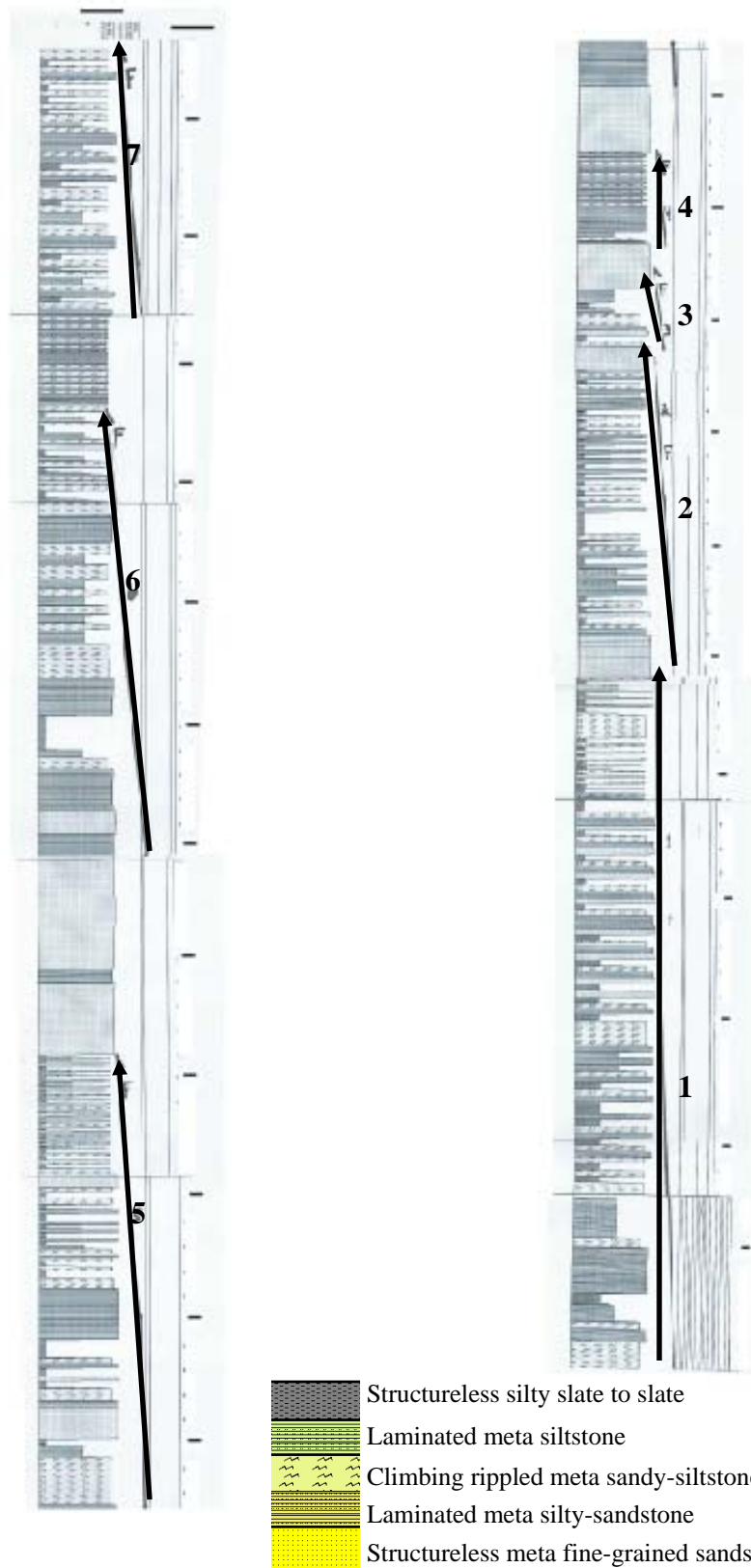Structureless meta fine-grained sandstone

Figure 3.6: Composite log with all the measured sections stacked on top of each other.
In total, there are seven cycles shown for the expanded section seen in Appendix IV.

3.4 LiDAR

All of the outcrops scanned gave three different reflected intensities (Table 6). These were high, medium and low intensities. If the image is not saturated with one intensity, then they represent the amount of quartz in the beds.

Table 10: Point cloud intensities and their representative quartz amounts.

Intensity	Description
High	Quartz >70%
Medium	Quartz 50%
Low	Quartz <30%

3.4.1 Near Point Pleasant Park Road

Point Pleasant Park road outcrop (Fig. 3.1) is 4.23 meters in height and is heavily covered by lichen. The co ordinates of the outcrop is 454689E 4941525N. The reverse image shows the outcrop covered by the lichen, however five beds can be seen in the outcrop. The bedsets range in thickness between 1-1.5m in thickness (Fig. 3.7). The image shows that the bedsets are laterally continuous within in the outcrop.
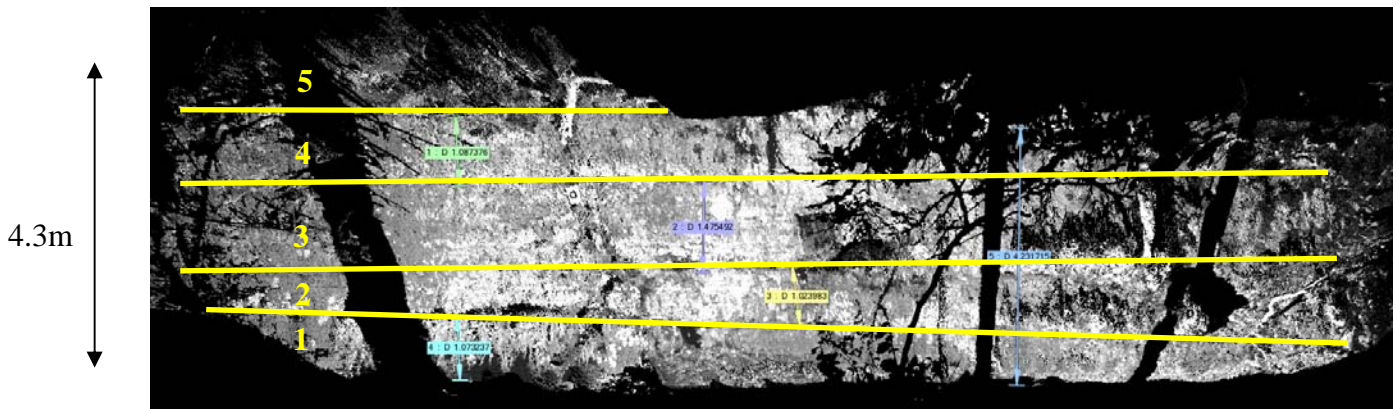

Figure 3.7: LiDAR image of the five bedsets ranging 1-1.5 meters thick. These packages are laterally continuous in this outcrop.

3.4.2 Black Rock Beach

The LiDAR image (Fig. 3.9) shows a definite variation in the intensities. The white data points show the light colour bedding that is laterally continuous. The beds are parallel to irregular, and range from 3-30cm, with a mean of 3 cm. The dark data points represent darker coloured bedding. The dark beds are similar in size and are parallel.

2.2 m

2.2 m

High intensity points showing laminae
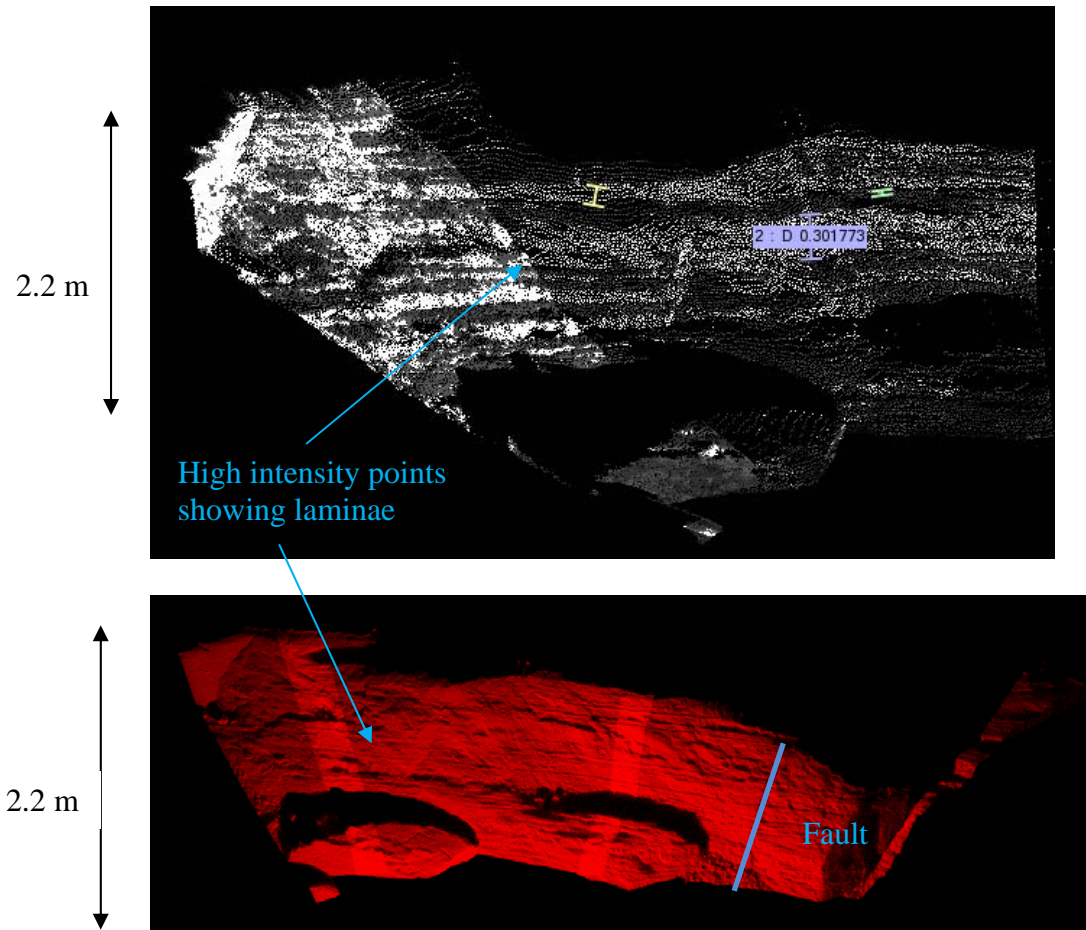
Fault

2 : D 0.301773

Figure 3.8: Images showing Black Rock Beach with the difference in intensities indicating the different lithologies present. Numbers on images are the bed thickness in metres.

3.4.3 Point Pleasant Battery

The outcrop (Fig. 3.9) comprises into two bed sets. The first bedset has a thickness of 40 cm while the other bedset has a thickness 13-19cm. The thicker bedset

shows no structures while the thinner bedset show some parallel laminations. At the very top of the outcrop there is a bedset that is 40 cm with five beds. Each bed is around 10 cm. This bedset is similar at the very bottom of the outcrop as the thickness is 36 cm and each layer is around 10 cm. Comparing the two bedsets, they are showing a fining upward succession. These layers can be seen laterally on the right of the outcrop, as well as the thick structureless sections.
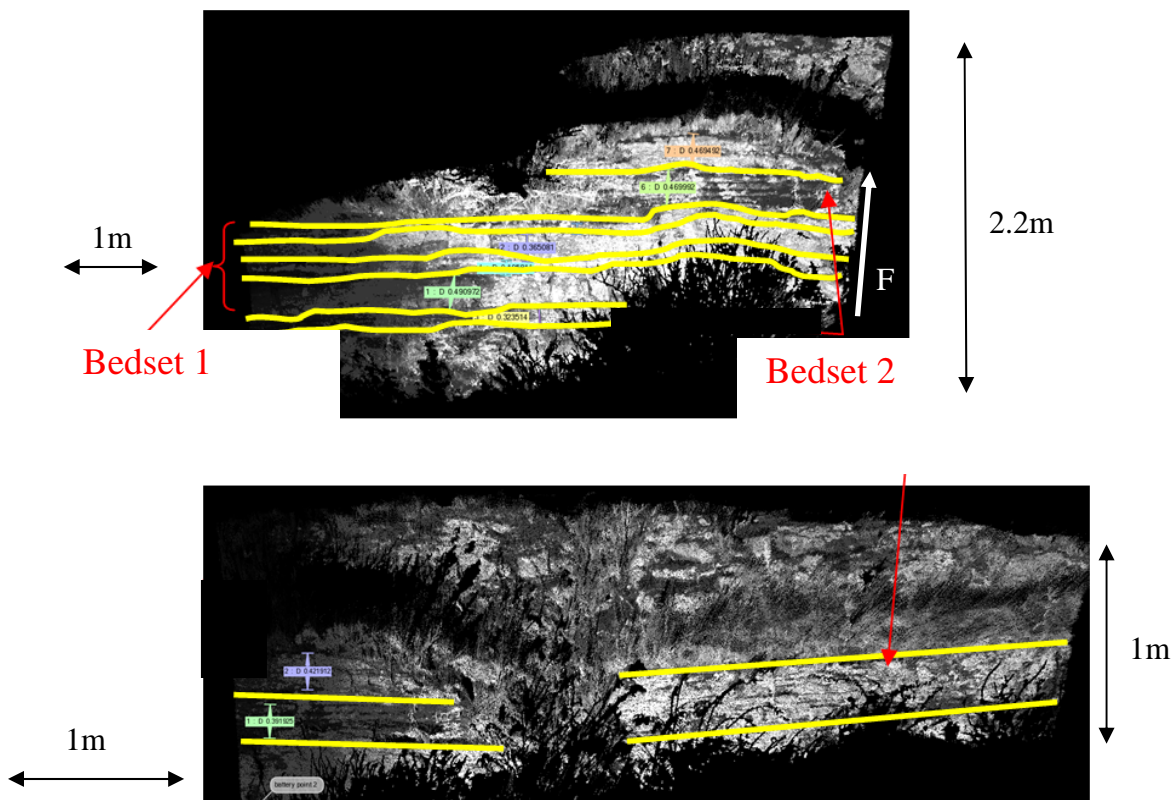

Figure 3.9: Point Pleasant Battery showing two bedsets. The outcrop is laterally continuous as seen in both images and is fining upwards. Numbers represent bed thickness in metres.

3.4.4 Sedimentological Type Section

The image (Fig. 3.10) shows the upper outcrop saturated with high intensity

points, making quartz ratios hard to determine. This becomes an indicator of using

LiDAR as an indicator of metamorphism on a local scale. Where there are some

differences in intensities, the outcrop showed the laminae. The laminae are parallel. The

intensities represent quartz and mica rich areas. The higher intensities are located at the

bottom off the outcrop and the outcrop becomes darker towards the top. This relationship

reflects the fining upward nature of the beds and the decrease in sand size (quartz) grains.

Increased metamorphism across the peninsula from the east to west also limits grain size

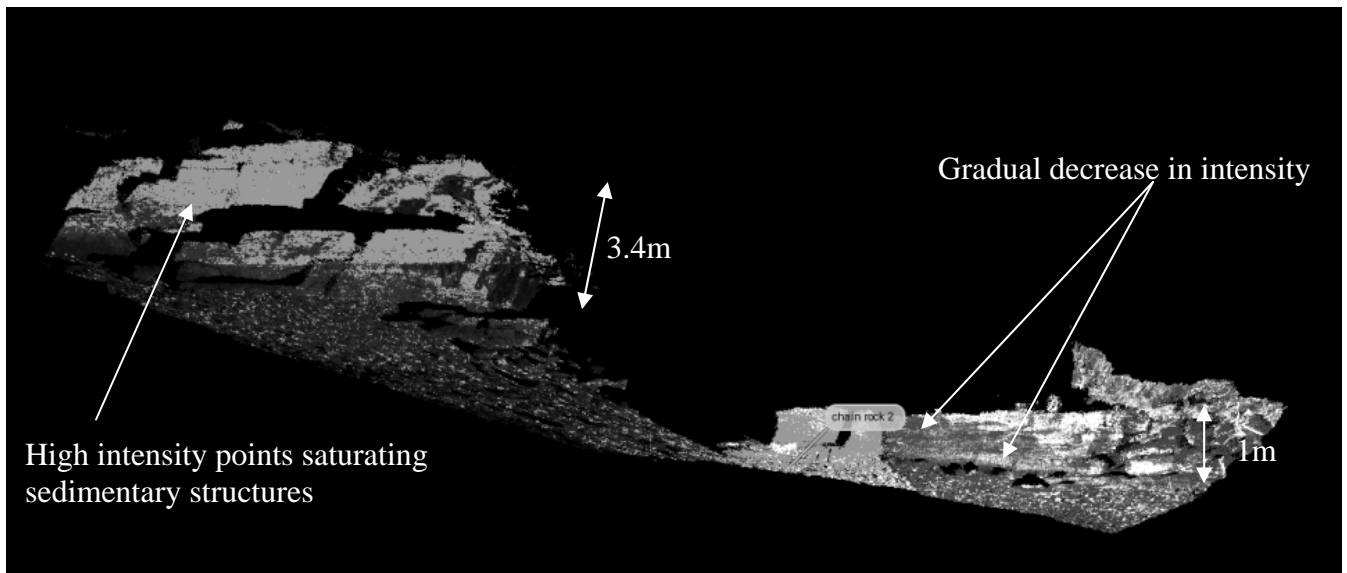identification and this may be a factor in the resultant LiDAR reflected intensities.

Figure 3.10: Image of the upper outcrop of the Type Section. This image shows that in areas one can see the intensities changing throughout the outcrop and while in other areas it is saturated with high intensity points.
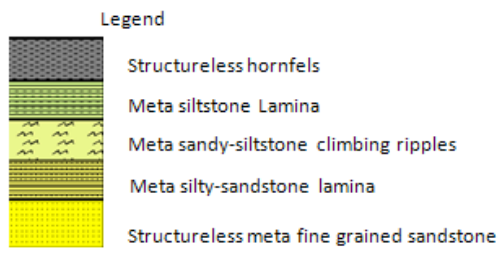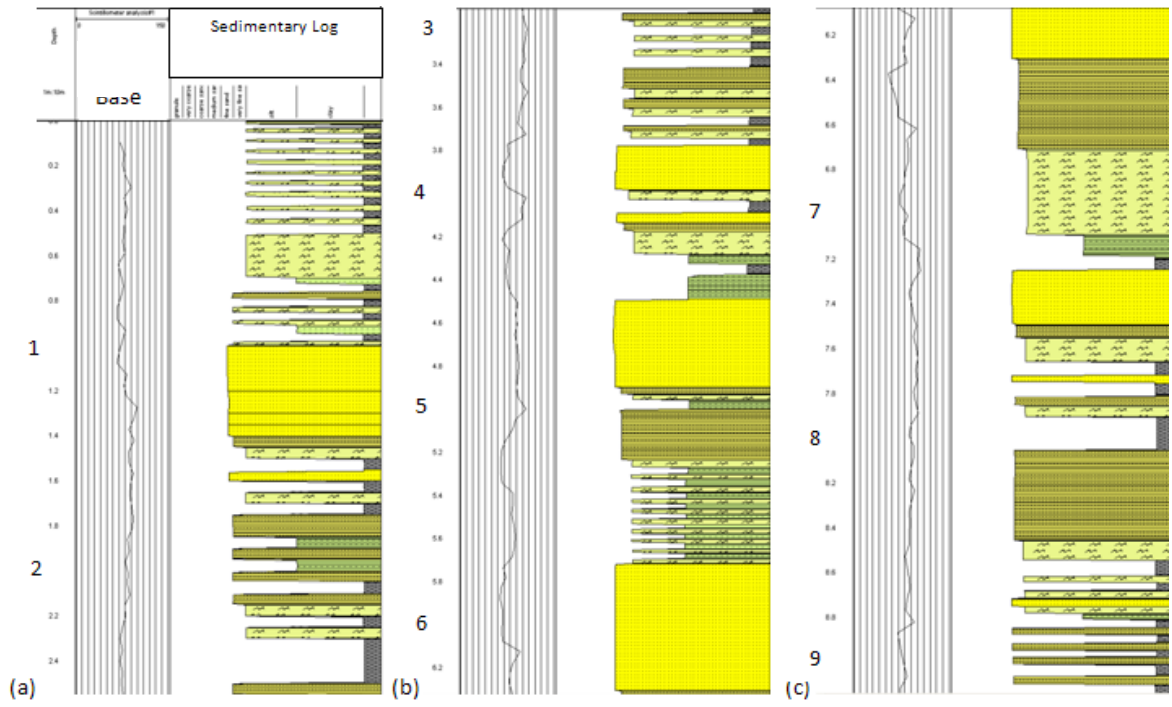
3.5 Scintillometer Analysis

Figures 3.10-3.13 illustrate the scintillometer measurements combined with the

outcrop lithologies on the measured section. Note, these images have been inverted so

that they represent a subsurface log of a core from a well. There was little change when

the API scale was changed to a smaller scale to try and enhance the character of the log trace.

3.5.1 Sedimentological Type Section

The scintillometer analysis (Fig. 3.11) shows a general fining-up succession, and the range is 69-109 API. There is also smaller scale coarsening upward cycles indicated by a decrease in API in three intervals. Gamma ray shows a range in API values and does fining upwards in some beds of the outcrops. There is also some relationship between the gamma ray and the lithology evident from gamma ray signature becoming less where blocky meta fine grained sandstone is present. However, the wireline also moves to the left in the presence of slate when it should be moving right. Minor interbedding in the outcrop is represented on the log signature.

Legend

- Structureless hornfels
- Meta siltstone Lamina
- Meta sandy-siltstone climbing ripples
- Meta silty-sandstone lamina
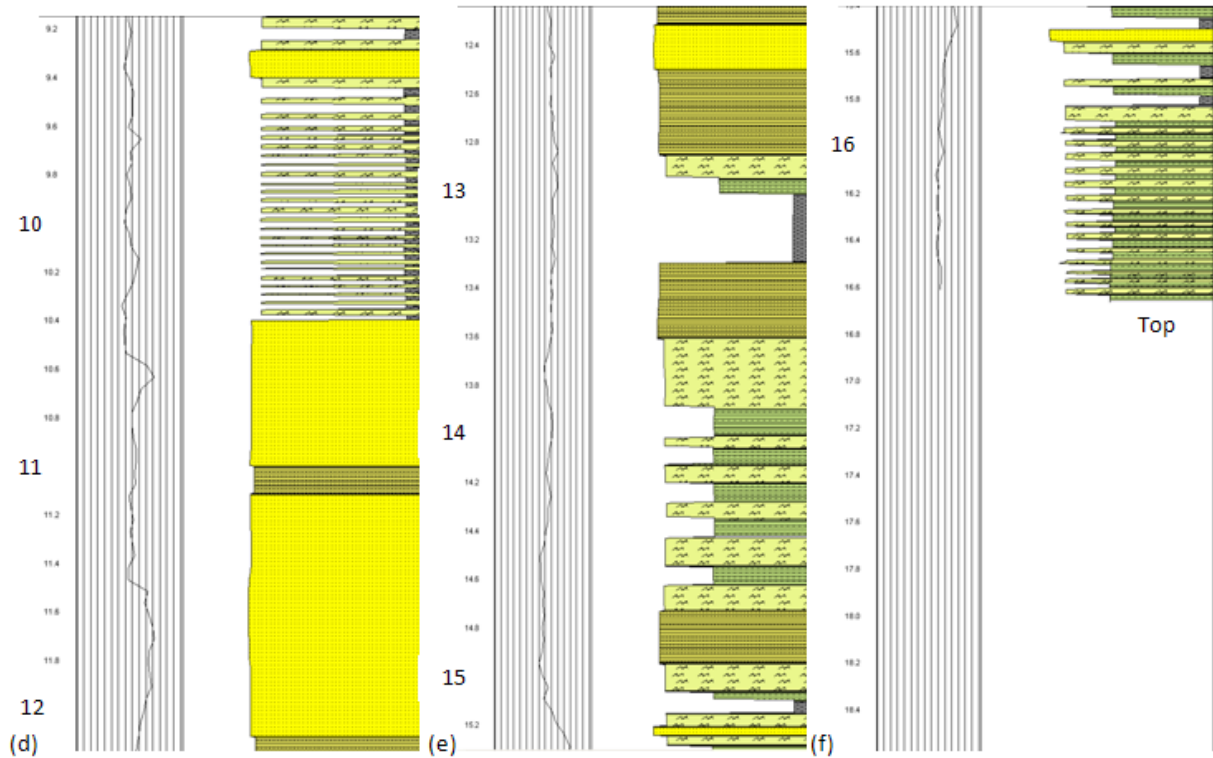- Structureless meta fine grained sandstone

Figure 3.11: Scintillometer analysis of the Type Section compared to the lithology of the outcrop. There is a general fining upwards sequence, and the range is 69-109 API. There is three fining upward cycles as the API decreases in three intervals. Gamma ray shows a range in API and does show some fining upwards in some of the outcrops, but there is no apparent relationship with the gamma ray and the lithology. Appendix V shows full version.

3.5.2 Point Pleasant Battery

The scintillometer analysis (Fig. 3.12) shows that there is little change between

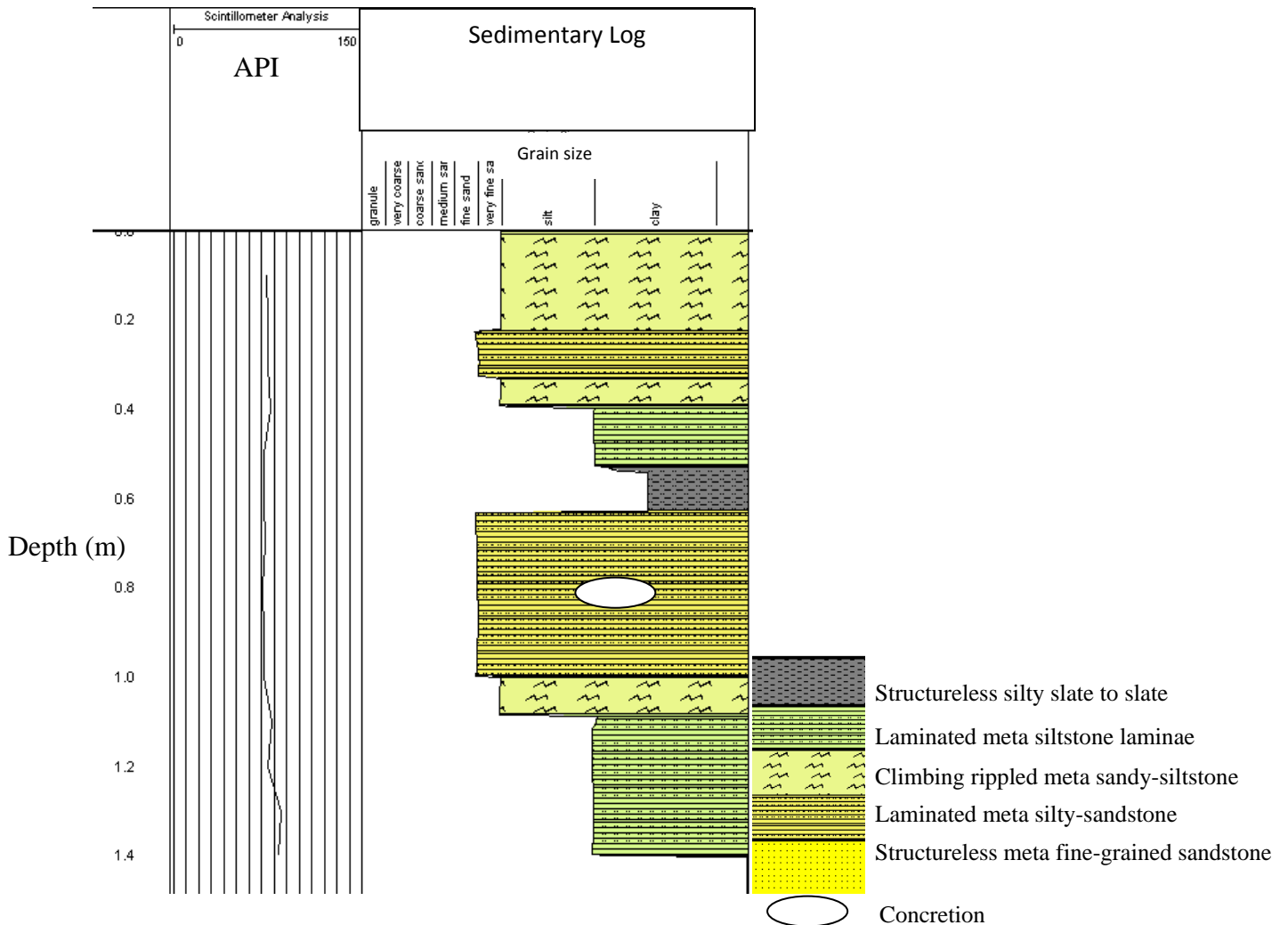the different layers on a 0-150 API scale. The range is between 71-83 API.

Figure 3.12: Scintillometer analysis of the Battery Point compared to the lithology of the outcrop. There is little change between the different layers on a 0-150 API scale. The range is between 71-83 API.

3.5.3 Black Rock Beach

The gamma ray (Fig. 3.13) shows that there is a general cleaning upward through the outcrop. The gamma ray ranges from 75-100 API. The API values are fairly consistent for 1.2 m, and from 1.2-2.2m there is a gradual reduction in gamma ray counts. In reality this shouldn't be happening as there is slate at the top of the outcrop, therefore there should be a higher gamma reading. The jaggedness of the wireline might indicate interbedding and interlaminations.
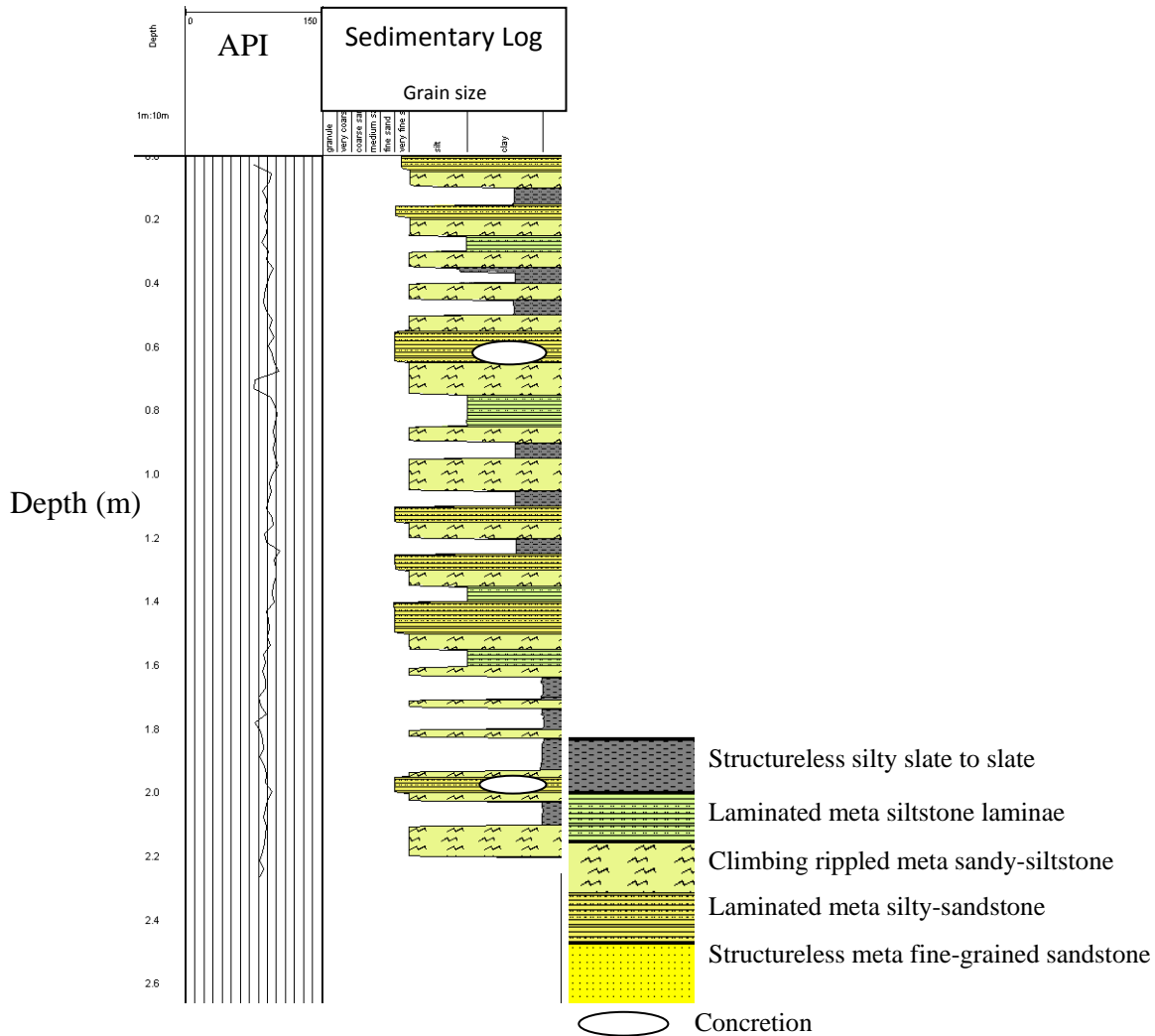
Figure 3.13: Scintillometer analysis of Black Rock Beach compared to the lithology of the outcrop. There is a general cleaning upward through the whole graph. The gamma ray ranges from 75-100 API. The API values are fairly consistent for 1.2 m, and from 1.2-2.2m there is a gradual reduction in gamma ray counts.

3.5.4 Sailors' Memorial Road

The scillometer analysis (Fig. 3.14) shows that it is coarsening upward and has a range is 68-95. This could be due to increased sand content which makes the interval 1.6-3.2m move to the left. The gamma ray log does not show the interbedding between the different lithologies.
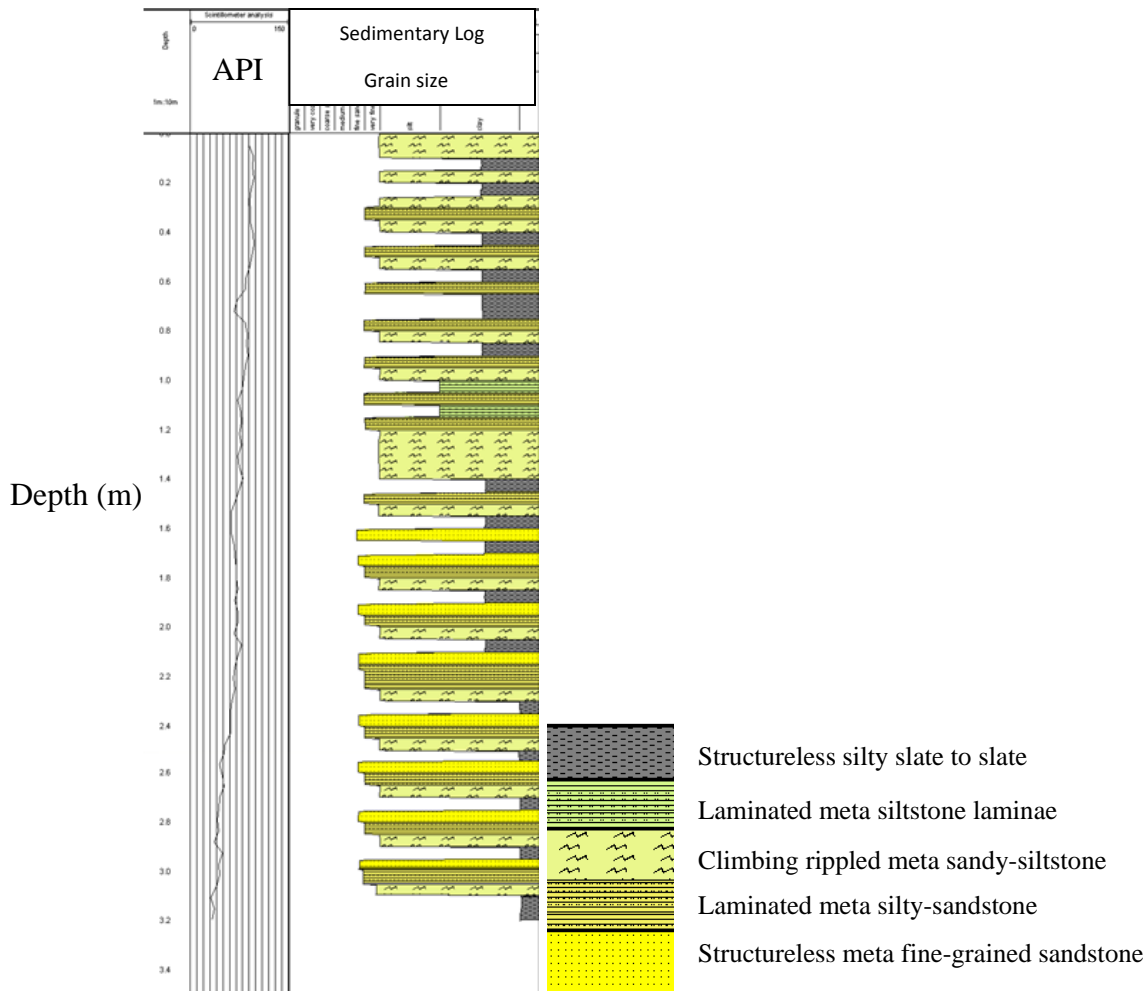
Figure 3.14: Scintillometer analysis of Sailors' Memorial Road compared to the lithology of the outcrop. There a gradual coarsening upward interval and has a range is 68-95. This could be due to increased sand content which makes the interval 1.6-3.2m cleaner. Gamma ray log does not show the interbedding between the different lithologies.

3.6 Petrographic Analysis

3.6.1 Laminated meta silty-sandstone with hornsfel (PPP04-03)

This thin section (Fig. 3.15) comes from the top of the Sedimentological Type

Section (Fig. 3.2) and shows the contact between the silty slate to slate and the meta silty

sandstone laminae lithofacies. The silty slate to slate layer is made up of 90% biotite, and

muscovite, and 10% quartz. The common secondary mineral is cordierite. Cordierite is a

product of metamorphism. The amount of cordierite present is related to the amount of mica.

The meta sandy siltstone climbing ripple lithofacies is made up of interbedded biotite, muscovite, and quartz. Quartz makes up 70% of the coarser-grain area and the grains have overgrowths, making accurate grain size measurements difficult. Cross-lamina are visible as the biotite, and muscovite layers outline these structures. Compared to some of the slides the biotite is coarse, enhancing the sedimentary structures. The laminae are separated by a scoured contact.
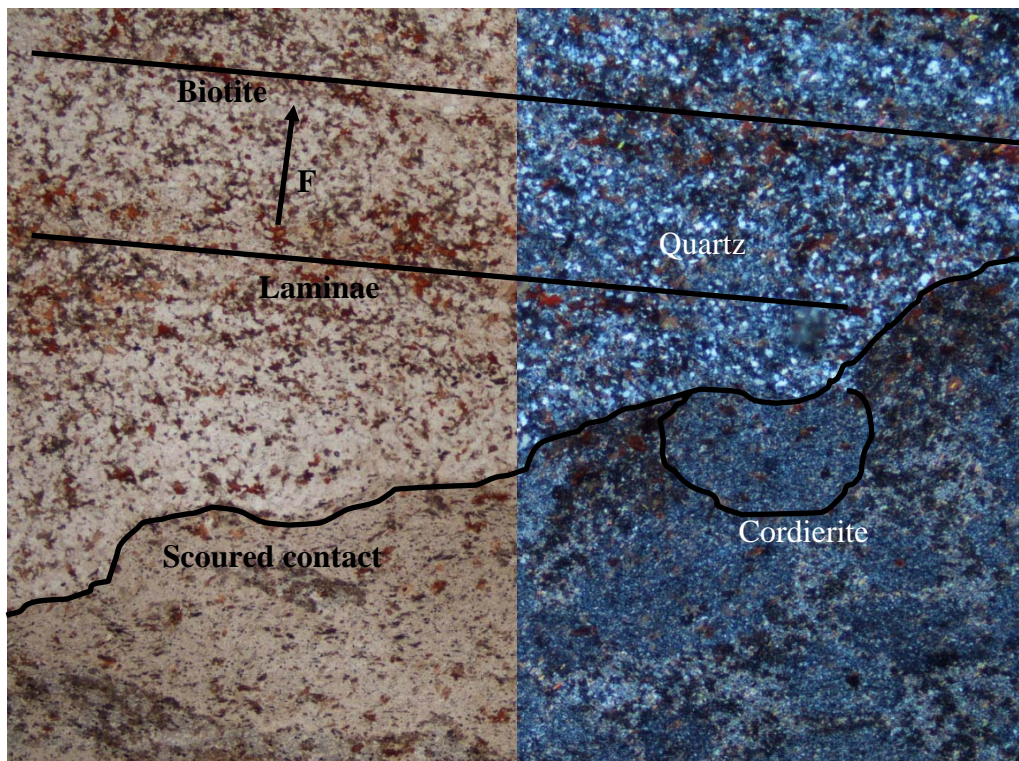

Figure 3.15: Thin section image of PPP04-03 in plane polarized light, and in crossed nicols. The scoured contact has cordierites which haven't completely developed due to the lack of biotite in the coarser component. The top left of the image is coarser grained than the bottom right. Laminae is discontinuous and the laminae in the bottom is barely visible. FIELD OF VIEW 6.25mm

3.6.2 Concretion (PPP04-04)

The thin section (Fig. 3.16) is made from one of the concretions, and comprise calcite, quartz, clinopyroxene, amphibole, titanite, zoisite, epidote, and garnet. In addition to calcite, the concretions are iron and manganese rich, (magnesite) with siderite. A sharp contact divides the concretion from the surrounding rock. The non-carbonate component of the slide contains some quartz but is rich in biotite.
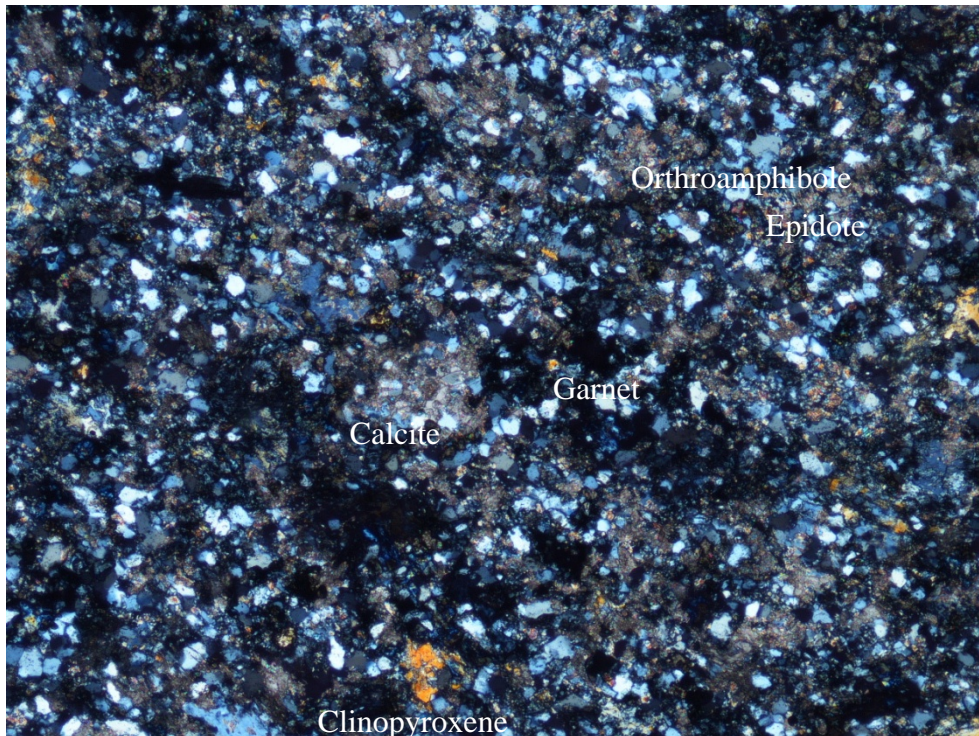

Figure 3.16: Image of PPP04-04 in cross nicols showing the different minerals found in the concretion. The thin section is made up of calcite, quartz, clinopyroxene, amphibole, titanite, zoisite, epidote, and garnet. FIELD OF VIEW 6.25mm

3.6.3 Laminated meta silty sandstone (PPP04-05a)

The thin section (Fig. 3.17) is from behind Point Pleasant Park Battery (Fig. 3.4) and represents the silty sandstone laminae and is made up of 65% quartz, 25% biotite, and 5% heavy minerals. Mica are also found surrounding the quartz, which preserves original grain size because it inhibits further quartz growth. The estimated grain size of

one of these quartz is 0.09mm (fine-grained). The heavy minerals are tourmaline and

zircon and these minerals are found together. The thin section also contains some

cordierite and pyrrhotite intrusions as secondary minerals. The cordierite is an alteration

of sheet silica and absorption of iron oxide. The pyrrhotite transformed from pyrite and

the mineral is elongated due to the cleavage. This thin section shows discontinuous

parallel laminae and cross laminae. The laminae show the grain size fining up,

suggesting waning current flow. The parallel laminae and cross laminae are easily

defined by the aligned mica. The heavy minerals like zircon and tourmaline also help
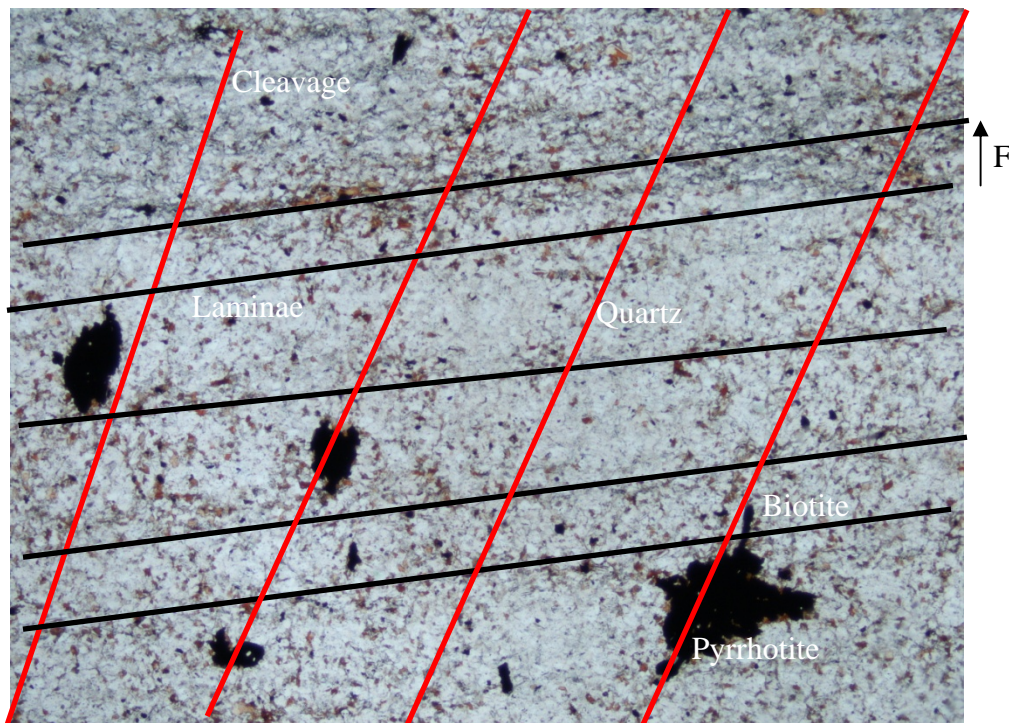
make up the laminae.

Figure 3.17: Image of PPP04-05a in plane polarized light. Highlighted from the lines
are the cleavage (70°) and the laminae. The laminae are defined from the mica present.
FIELD OF VIEW 6.25mm.

3.6.4 Climbing rippled meta sandy-siltstone (PPP04-05b)

This thin section comes from the same outcrop as the PPP04-05a (Fig. 3.4), however this thin section shows cross laminae. This thin section represents the meta sandy-siltstone climbing ripple lithofacies. It contains the same minerals found in 5a, but there is more mica than quartz. The thin section is made up of around 40% quartz, 55% biotite, and 5% heavy minerals. The heavy minerals are tourmaline and zircon and they are found together. These minerals are detrital and are important because they have been unaltered from the metamorphism so a grain size estimation could be made. The thin section contains more cordierite and the quartz is finer grained than 5a. The quartz is 0.04mm (very fine grained). Cleavage is visible from the elongated pyrrhotite and has an angle of 70°.

3.6.5 Concretion (PPP04-05)

The thin section comes from one of the concretions found in Point Pleasant Battery (Figure 3.4) and is made up of carbonate minerals. The dominant mineral is calcite, with some manganese (magnesite). Non-carbonate minerals include garnet, some sulphur oxides, and orthoamphiboles. The calcite surrounds and encloses the other minerals, suggesting that the calcite is secondary. There is a sharp contact between the concretions and the surrounding beds, evident from the biotite truncated at the contact. No sedimentary structures are found in the thin section.

3.6.6 Laminated meta siltstone and climbing rippled sandy-siltstone (PPP04-06)

The thin section (Fig. 3.18) represents the meta siltstone lamina lithofacies and contains 30% quartz, and 70% biotite. Heavy minerals are lacking in this thin section and there is a high amount of cordierite. The quartz is finer grained, and cleavage is seen,

due to crenulation. The crenulation is evident from biotite minerals stacked on one another. This modifier is usually found in fine-grained rocks (Jamieson, Pers. Comm., Novemeber, 2009). The micas are coarser than micas in PPP04-04 and PPP04-30.

This slide also contains the meta sandy-siltstone climbing ripple lithofacies evident from the coarser grains and higher amount of quartz. The amount of quartz to biotite changes to around 60% quartz, 30% biotite, and 10% heavy minerals. The heavy minerals are zircons and tourmaline and are localized. Due to the coarser grain size, the cleavage is less apparent. Cross-laminae is visible, enhanced by the biotite content.

Fine-grained

Cross ripple laminae

Heavy minerals

Cross ripple laminae
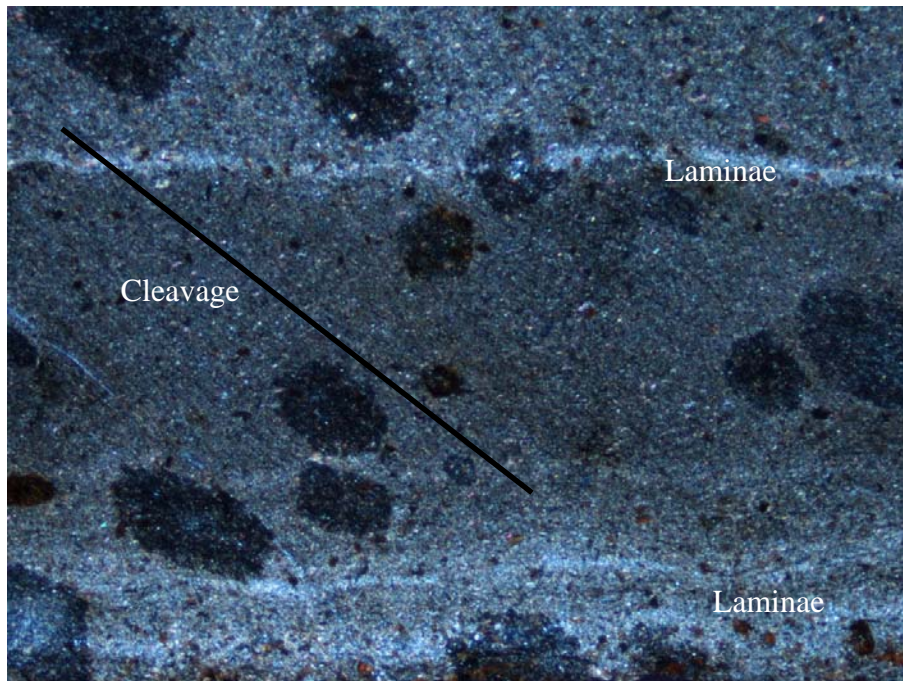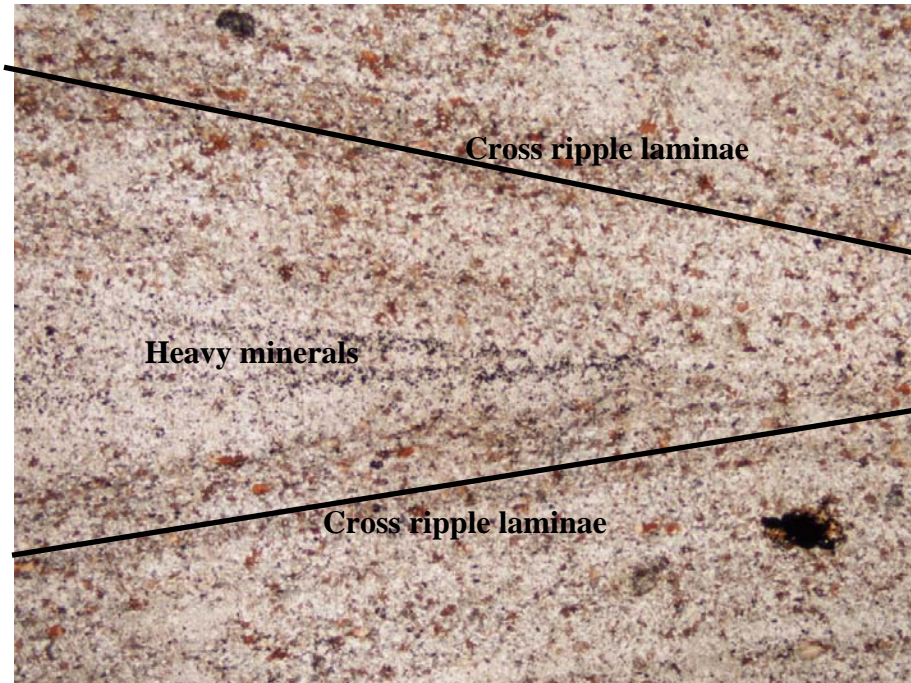
Coarse grained

Figure 3.18: Images of PPP04-06 in plane polarized light, and crossed nicols. They show laminae and a change in grain size. These images are located in different areas of the thin section. FIELD OF VIEW 6.25m.

3.6.7 Laminated meta siltstone and laminated meta-silty sandstone (PPP04-09)

The thin section (Fig. 3.19) represents the meta silty sandstone lithofacies and it contains 60% quartz, and 40% mica found in Black Rock Beach outcrop (Fig. 3.3). The grain size of the quartz is around 0.07mm (fine-grained). Heavy minerals are rare or not present in the slide. Pyrrhotite is disseminated throughout the slide, while cordierite is found within the mica rich layers. Laminae are evident where the mica and quartz are interlaminated. The meta-sandstone is interlaminated with a silty layer. Cleavage is less visible and steeply dipping 70°.
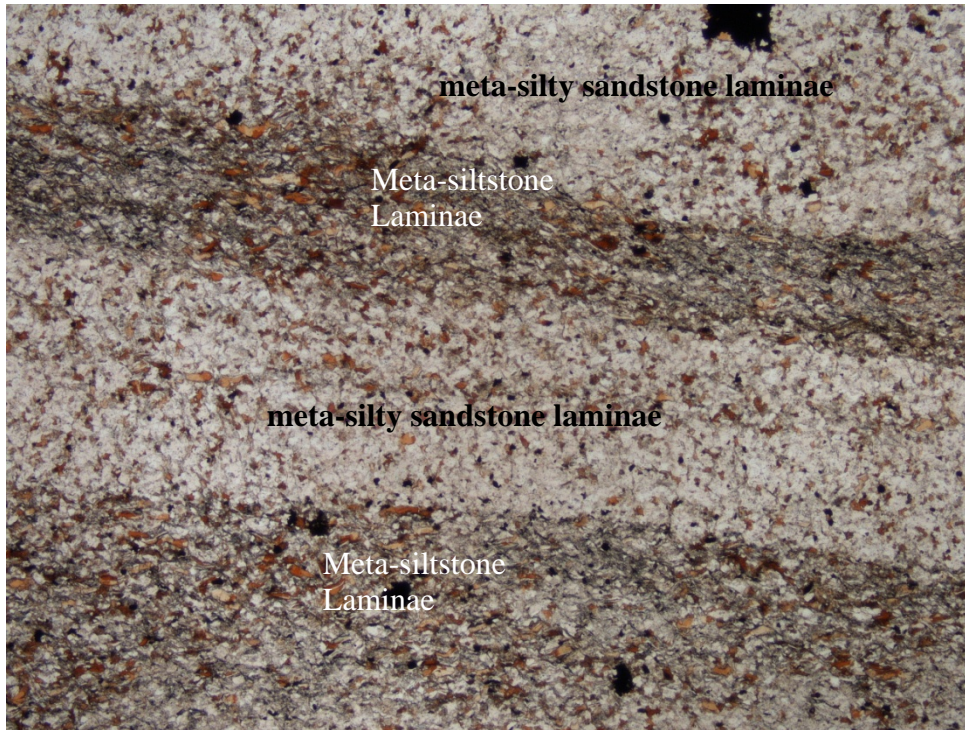
Figure 3.19: Image of PPP04-09 showing interlaminae of meta-siltstone and meta-sandstone. The mica grains in the slide are 0.03mm larger than the ones found in the thin sections from Black Rock Beach and behind Point Pleasant Battery Point. FIELD OF VIEW 6.25mm.

3.6.8 Structureless silty slate (PPP04-15)

The thin section (Fig. 3.20) represents the structureless silty slate lithofacies and contains mainly chlorite, cordierite, muscovite, and biotite. There is a presence of chlorite from a reaction between biotite and muscovite. The cleavage is also visible, but sedimentary structures are not present.
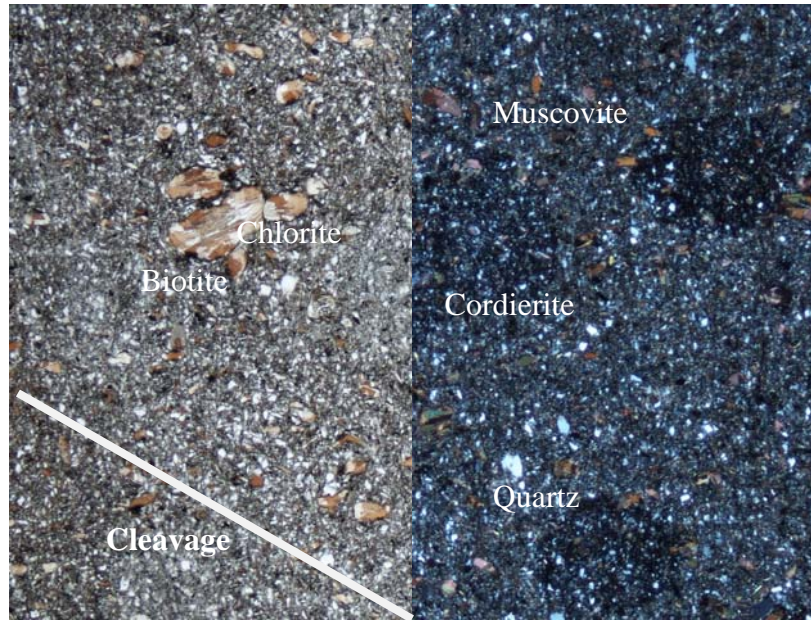
Figure 3.20: Thin section showing PPP04-15 in plane polarized light and cross nicols. The section shows mainly mica, cordierite and very little quartz. The section also shows no sedimentary structures but the cleavage is present as a product of metamorphism.

3.6.9 Meta sandy-stilstone climbing ripples and meta siltstone (PPP04-30)

The thin section (Fig. 3.21) is a sample from Black Rock Beach outcrop (Fig. 3.3) and contains clastic and carbonate components. The clastic component is made up of two different lithofacies; the meta sandy-siltstone climbing ripples, and meta siltstone lithofacies, divided by a scoured contact. Both lithofacies are made up of quartz and biotite, but the ratio of quartz and biotite varies. In the climbing rippled meta sandy siltstone lithofacies, there is 60% quartz and 40% biotite. The grain size of the quartz is 0.04mm (very fine-grained). The lithofacies is made up of climbing ripples that are divided into quartz and biotite laminae. The meta siltstone lithofacies is made up of 40% quartz and 60% biotite and contains siltstone and sandy-siltstone laminae. Grain size of the quartz is 0.01mm (silt).

Meta sandy-siltstone
climbing ripples

Contact

Meta-siltstone

Meta-siltstone

Artifact
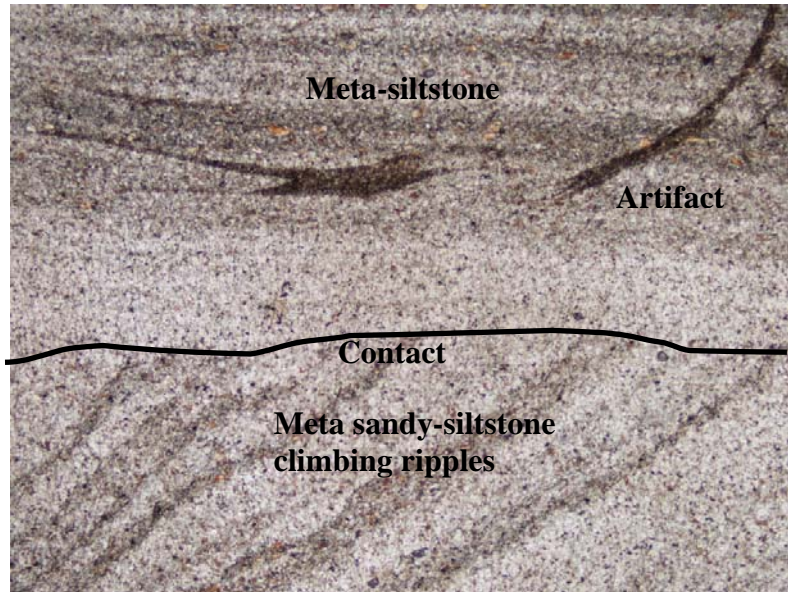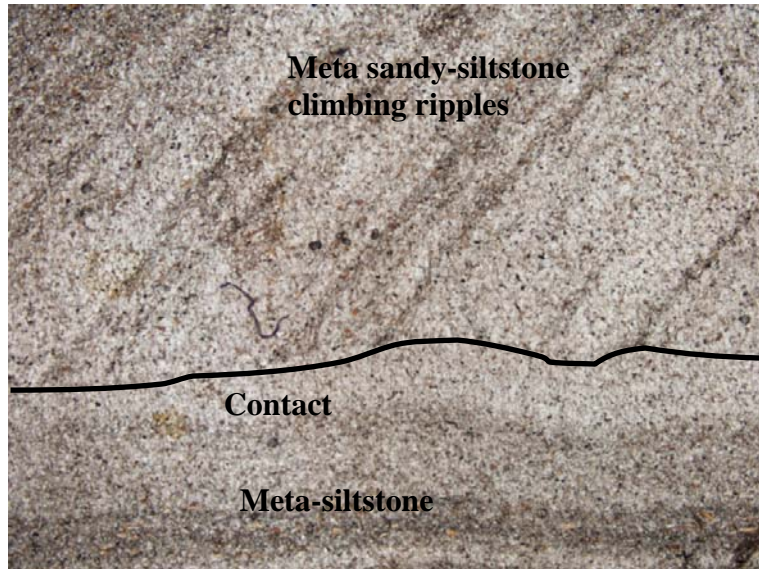
Contact

Meta sandy-siltstone
climbing ripples

Figure 3.21: Image of PPP04-30 showing the sharp contact between the meta siltstone and the meta sandy siltstone climbing ripples lithofacies. FIELD OF VIEW 6.25mm

3.7 Paleocurrent Analysis

Paleocurrent analysis was done on climbing ripples and corrected on steronet. Climbing current ripples found on the surface of the bedding plane on the outcrops, were corrected using a stereonet (Fig. 3.22) and show that the paleocurrent flowed towards the north west. 310 ± 22°.
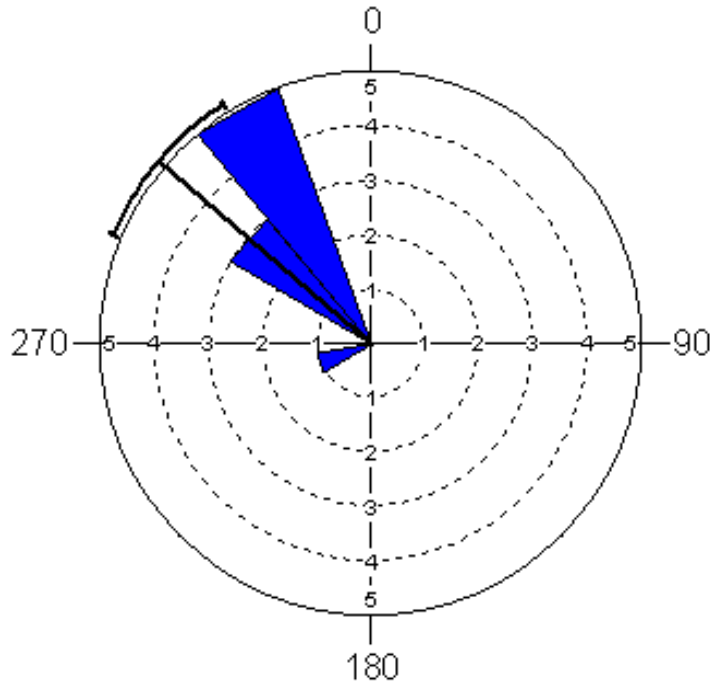
Number of observations	9
Mean Vector	310°
Circular Standard Deviation	22°

Figure 3.22: Rose diagram shows the current orientation of the climbing ripples in Point Pleasant Park. The figure shows that the average orientation is 310 ± 22°.

3.8 Summary

The Sedimentological Type Section contains structureless meta fine-grained sandstone, laminated meta silty-sandstone, climbing rippled meta sandy-siltstone, laminated meta-siltstone, and a structureless silty slate to slate lithofacies with some

lithofacies more abundant than others. There is a pattern of thinning and thickening in the bedding in the outcrops. Where bedding is thick, meta structureless sandstone, and laminated meta silty-sandstone dominate, and as the bedding becomes thinner meta siltstone laminae and structureless silty to slate lithofacies dominate. This cycle is apparent in the Sedimentological Type Section. Paleocurrent measurements from surface exposures of current ripples show an orientation of 310 ± 22°.

Gamma ray shows a range in API and does show some fining upwards in some of the outcrops, so there is some relationship between the gamma ray and the lithology. This is evident when there is massive beds of fine grained meta sandstone present and the jagged log pattern due to interlamination and bedding.

Thin sections show that the outcrops are made up of quartz, biotite, muscovite, heavy minerals, cordierite, and pyrrhotite. The lithofacies show characteristics in outcrop as well as in thin section. Any slide with a lot of cordierite contained a high amount of mica. The variation in metamorphic grade from east to west is evident seen in the outcrops across the park which impacts grain size measurement on the north west area of the park.

4. <u>Discussion</u>

        The lithofacies found in the outcrops can be interpreted as the divisions of the Bouma sequence. The structureless fine-grained meta sandstone, laminated meta silty-sandstone, climbing rippled meta sandy-siltstone, laminated meta-siltstone, and structureless silty slate to slate lithofacies are the lithofacies found in the outcrops. The lithofacies are interpreted as the T_a-T_e divisions of the Bouma sequence. The lithofacies or divisions show gradual, scoured and sharp contacts. This can be seen in the measured sections particularly in the Type Section and the upper half of Sailors' Memorial Road Section, and in the petrographic thin sections.

        The length and thickness of the lithofacies vary and the variation of the length is due to the limited extent of the outcrop, obscured by vegetation or truncated due to outcrop erosion. The length of these beds can be extrapolated for a further distance. Many of the outcrops contain two or three lithofacies. The thickness of these lithofacies can vary, as seen in Figures 3.5 and 3.7. LiDAR images show bedsets that represent fine grained sand-rich lithofacies that break easily on the mica rich beds. In Figure 3.7, a thinning upward interval can be seen in the image which represents a fining up cycle. The outcrop is coarser grained while bedsets made up of small beds are evident at the top due to an increase in the mica which also indicates a fining upward bed cycle. The lack of fine-grained sandstone could be due to the coarser sediments not being deposited on the overbanks as the coarser material will be deposited in channels. Rare, starved current ripples suggest a lack of coarser grained sediment during deposition.

 Figures 3.6, 3.7, and 3.8 show that differences in LiDAR intensities could be from the ratio of quartz to mica where the quartz-rich areas have a higher intensity and mica-rich

layers have a lower intensity. It is recommended that work continue on calibrating lithology and lithofacies to LiDAR intensity, as this can provide a rapid method for characterization outcrops, particularly where they are inaccessible for constructing measured sections.

The outcrops and the petrographic sections show that the bulk composition of these outcrops is quartz, biotite, and muscovite, cordierite, with accessory minerals like tourmaline, pyrrhotite and zircon. Measured outcrops found on the east side of the park (Fig. 3.1) were not as metamorphosed as the outcrops on the west side (Fig. 3.1 and Fig. 4.1).
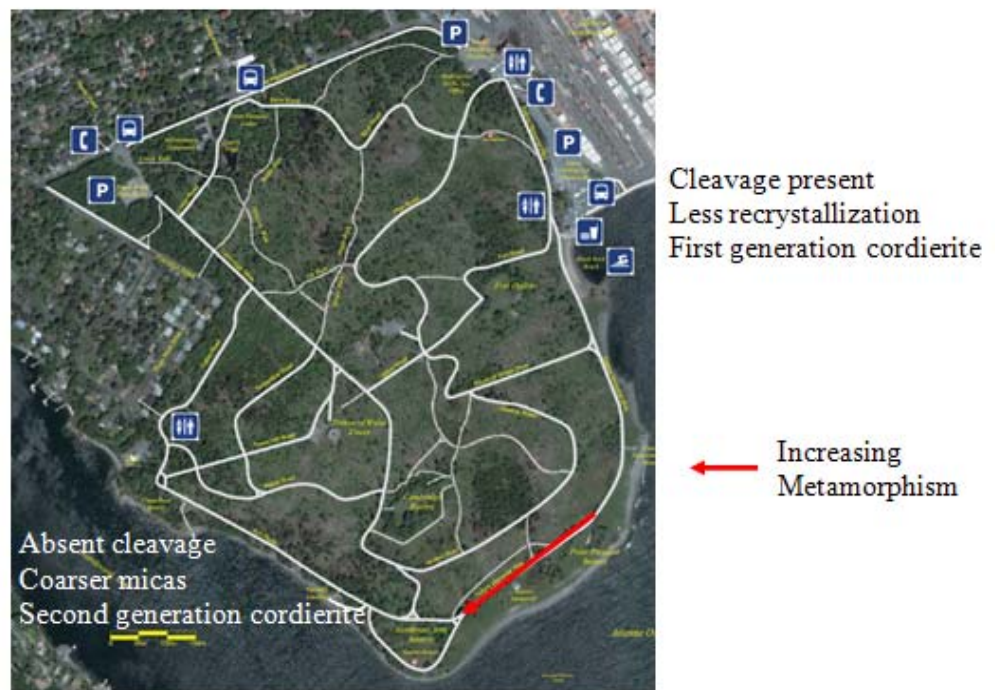

Figure 4.1: Map of Point Pleasant Park and the direction of increased metamorphism (Point Pleasant Park, 2009).

First generation formation of cordierite is seen in the outcrops on the east side of the park. Evidence of second generation formation of cordierite due to the halo that is formed around the cordierite, and coarser grains of biotite on the west side is due to the

intrusion of the South Mountain Batholith immediately to the west of the North West Arm (Fig. 1.3). This has implications on how certain outcrops can be measured and observed. The degree of metamorphism plays an important role because affected grain size in the outcrops determines clarity of sedimentary structures. The outcrops found on the east side of the park contain quartz grains that can be measured to give a relative grain size. The outcrops on the west side of the park have the majority of the quartz recrystalized impeding grain size measurements. The enlarged biotite crystals help emphasize the sedimentary structures on the west side of the park. Care must be taken as tectonic structures in the outcrops can be interpreted as sedimentary structures. There are beds in the outcrops that appear to contain ripples, but are actually boudinage structures and can also be seen in thin section. Some thin sections show crenulation. These features can form structures that could appear as current ripples at outcrop scale and care must be taken when determining true physical sedimentary structures for reading paleocurrents.

The scintillometer analysis shows a limited relationship, except in some areas where there are beds of fine-grained meta sandstone. Most of these outcrops are made up of thinly bedded layers which do not show a very big change in grain size. The range in grain size is from fine-grained sandstone to silty-clay so the range in the quartz grain size is not large. Some of the gamma ray log signature are 'ratty' or jagged which indicates interbedding and interlamination of the strata. With increased metamorphism on the western outcrops, the scintillometer was not able to distinguish lithology with great clarity. For example the scintillometer analysis of the type section shows a coarsening upward pattern when the lithology at the top of the measured section comprises slate.

This could be due to thorium, potassium, and uranium leached out from fluids during metamorphism and settling in the more porous lithologies like the sand rich laminae, producing a higher gamma ray signal in these laminae and beds.

Data plotted on the rose diagram shows that the paleocurrent flowed towards the north west. This result is comparable to paleocurrents recorded in outcrops on Tancook Island (Waldron, 1987; 2009); and from Harris and Schenk's (1975) regional observations. This suggests that deposition of the sediments comprising the Goldenville Group and the Bluestone Formation flowed in a similar direction on the passive margin.

The depositional setting of the outcrops have been ambiguous. Harris and Schenk (1975) suggested the Halifax Group was deposited as the distal part of a turbidity flow and perhaps as overbank deposits (Fig. 4.1). Although not the same stratigraphic interval, Scott (2003) from his work on the Tancook Formation, interpreted the Tanbrook Formation sediments as coastal mud flats with brackish influence, based on foraminiferal data.

With the lack of fine-grained sandstone and the dominance of the finer grained divisions in the Bouma sequence, there are two possible depositional models that could be represented. These are, 1) the distal part of the fan lobe and, 2) overbank and levees of a submarine channel, which were described in Chapter 1. The Bluestone Formation could be from the distal part of the fan lobe, similar to the Jackfork Group, in Arkansas. Fine grained material has been interpreted as distal material (Slatt et al., 1997). However, studies done by Kirscher and Bouma (2000), Basu and Bouma (2000), Schwarz and Arnott (2007), and Piper (2010) and the lithofacies in the outcrop suggest that the depositional analogue for the outcrops is levee and overbank deposits (Fig.4.2).
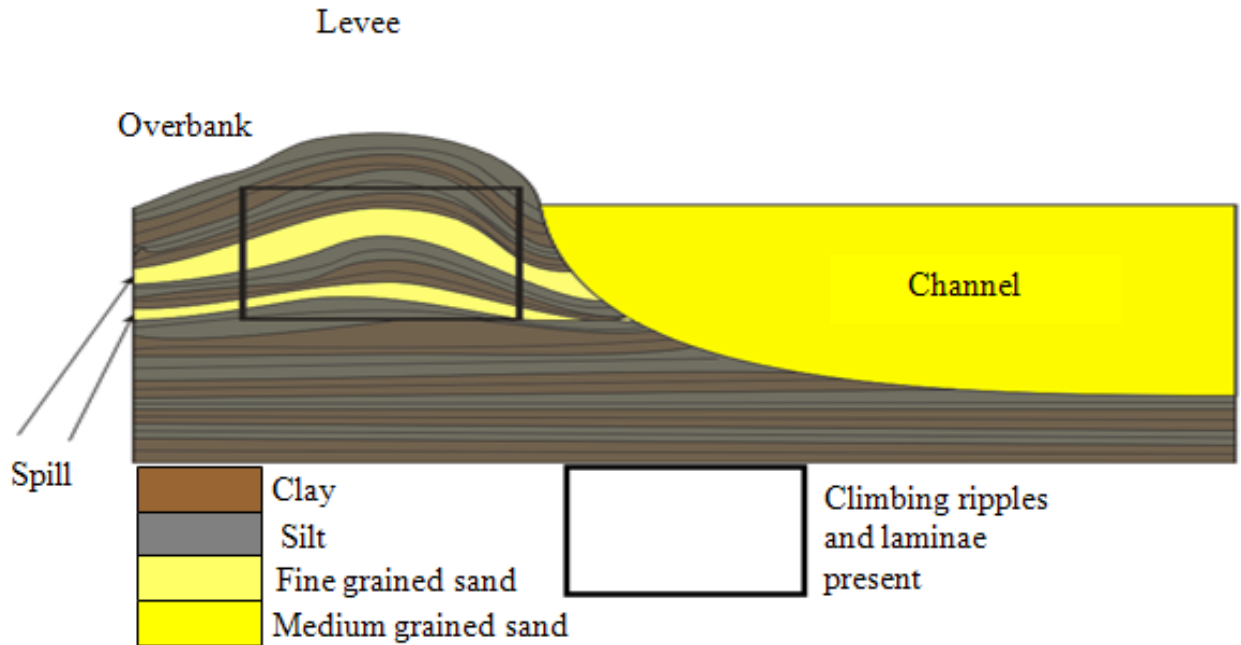
Figure 4.2: Schematic cross section of levee and overbank deposits adjacent to channel deposits. Deposits mainly made up fine grained laminae and climbing ripples with intermittent massive fine grained sandstone. Flow of turbidite is adjacent to cross section. (Modified from Basu and Bouma, 2000; Roberts and Compani, 1994).

Lithologies and sedimentary structures seen in the outcrops are similar to the characteristics in analogues in Tanqua Karoo, South Africa (Kirschner and Bouma, 2000; Basu and Bouma 2000). Kirschner and Bouma (2000) recorded laminated siltstones and observed sandstone with climbing ripples was a good indicator of interchannel deposits. They noted that any sandstone present was thinly bedded (Kirschner and Bouma, 2000), similar to the outcrops observed at Point Pleasant Park. When Basu and Bouma (2000) examined outcrops in the Tanqua Karoo, they concluded that the presence of climbing ripples and laminated siltstone indicated overbank and levee deposits. They explained the

occasional presence of sandstone as originating from the lobe spilling coarser

material onto the overbanks. This might explain the presence of the structureless

meta fine-grained sandstone in the measured sections. Furthermore, Mitchum and

Wach (2002) interpret the overbanks in the levee-channel complexes in the fans

down dip from the Niger Delta as comprising sandstone. Schwarz and Arnott

(2007) concluded from observations on thin bedded, fine grained laminated,

climbing rippled sediments in the Issac Formation, Castle Creek, British

Columbia that these came from inner bend levees and overbanks. Studies done on

core from the Lower Cretaceous Tantallon M-41 well (Piper et al., 2010), show

similar lithofacies, and the dominance of the finer grained divisions of the Bouma

sequence. Piper et al. (2010) believed that the dominance of the siltier lithofacies

and the lack of the sandier lithofacies are characteristic of fine-grained
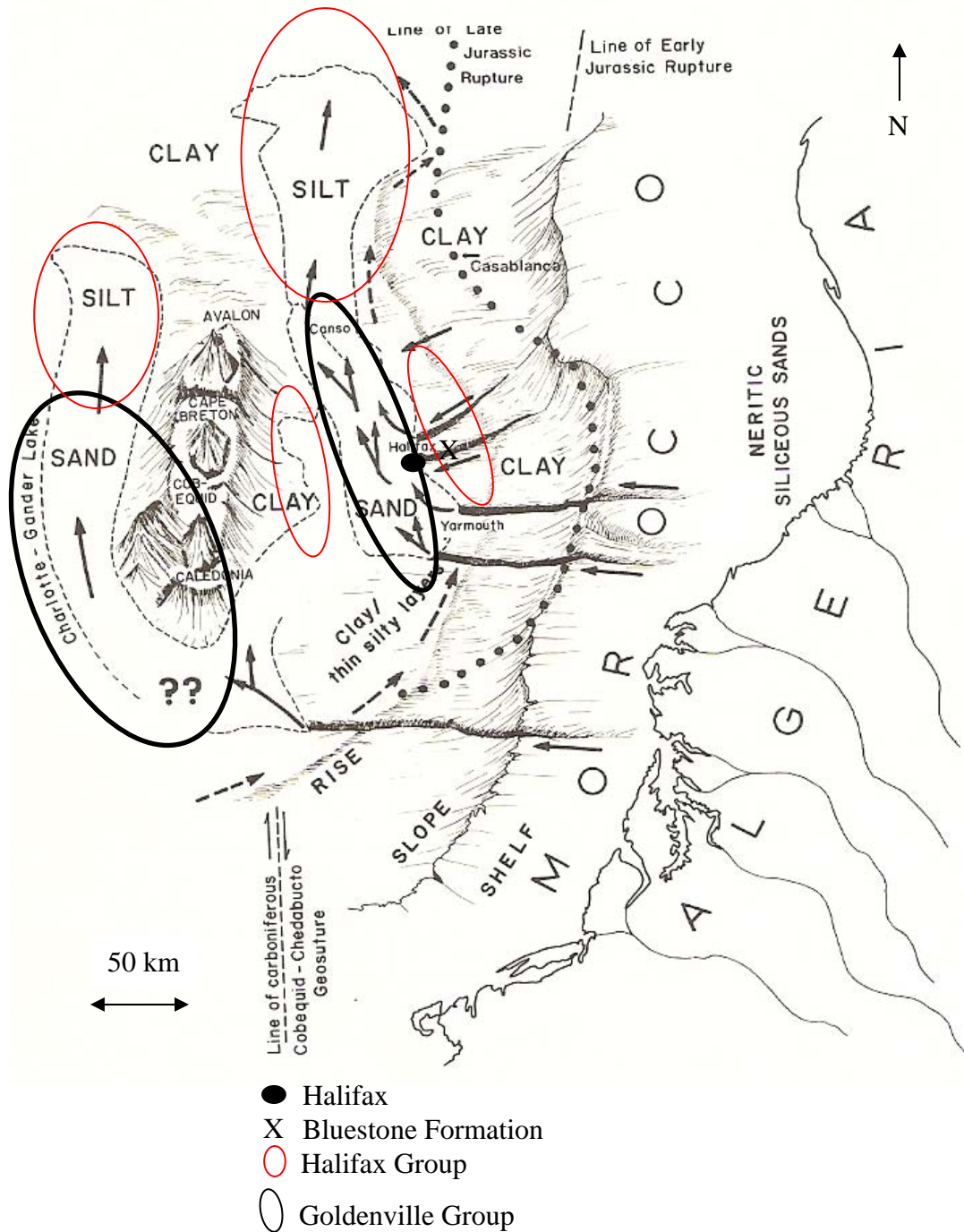
hyperpyncal turbidites.

Figure 4.3: Location of the Goldenville and the Halifax groups and the location of Halifax (Modified from Harris and Schenk, 1975). Diagram suggests that he city of Halifax was located on the overbank of the submarine channel. The Halifax Group is also located in the distal component of the turbidite shown in the red ovals. The Goldenville is represented by the sand is more proximal to the source. The flow is orientated the same direction seen in the outcrops.

Micropaleontological analysis provides another interpretation of the depositional environment. Scott (2003) suggests these sediments were deposited in an estuarine/ marsh environment based on the presence of *Trochammina* (forams) found in slate of the Halifax Group in Clayton Park, Halifax. This type of fossils would not survive in a deepwater environment deposited by turbiditic processes (Scott, 2003). The Point Pleasant outcrops of the Bluestone Formation do show physical sedimentary structures and a facies association indicative of deep basin turbiditic processes and an absence of shallow or estuarine processes such as wave ripples and tidal indicators such as neap/spring tidal bundles. Furthermore, turbidity is a process and not an environment although this association is often blurred in the literature. Turbidite deposits could have been sourced from an estuary and then transported downslope.

The Bluestone Formation can be used as a depositional analogue for petroleum exploration and development with application to conventional and unconventional plays. The Sedimentological Type Section shows 1 m fine grained sandstone capped by a silty bed that could act as a baffle or barrier to fluid flow. These beds do not appear to be laterally continuous over large distances and these sandstone beds may pinch out to form a stratigraphic barrier to flow or trap. The Bluestone Formation may be applied as an analogue for a shale gas production as most of the outcrops are made up of silt and clay. The claystone intervals between the measured sections could be an analogue for a gas source generate thick packages of claystone if organic rich. This is very similar to the Triassic Motney shale play in north west British Columbia, produced from low density turbidites and today is a hotspot for shale gas exploration and development. Other fields that produce from similar depositional environments include the Baudroie Marine and

Baliste fields in West Africa, Bud and Teak fields in the Gulf of Mexico, and the

Novillero field in Mexico.

5. Conclusions and Recommendations

The Bluestone Formation outcrops at Point Pleasant Park show evidence of a long and complex geological history. With the use of standard and new technologies, observations and analysis demonstrate these outcrops contain lithofacies that are characteristic of the divisions of the Bouma sequence. There are several cycles

Comparison with the outcrop at Tanqua Karoo and in core from the Tantallon M-41 well suggest that these sediments were deposited as overbanked low density turbidites. Thin sections show that the lithofacies have their own characteristics in thin section and the growth of cordierite indicates the protolith was mud rich. Metamorphism also helped enhance the sedimentary structures but made it hard to record an accurate grain size on the western side of the park (Jamieson, Pers.comm).

Studies offshore Nova Scotia, and South Africa show similar lithofacies and the location of the Bluestone Formation prior to the rifting and folding association with the Acadian Orogeny in the Devonian and Jurassic (Piper et al., 2010; Schenk, 1975). Paleocurrents show that as the sediments were being deposited, turbiditic flow was north west, confirmed by earlier regional studies (Waldron 1987; Schenk 1975).

If we conclude that these outcrops were deposited as overbank deposits, where are the associated channel sands? These sands are not seen within or near the park so more work needs to be done to locate the channel sands that came from the same turbiditic flows that these finer grained sediments originated, or are the sediments from distal flows down dip or lateral to channelied inner for deposition.

The study shows that application of new techniques like the LiDAR help define some of the architectural elements, however standard methods like measured section and

sedimentologic and petrographic analysis are paramount to any study to provide the ground data for calibration of LiDAR and scintillometer analysis.

Recommendations for future study include completing a similar study on the Cunard Formation and the Taylors' Head Formation of the Goldenville Group to compare the sedimentological characteristics of the low density turbidities between the Bluestone and the Cunard with high density turbidties of Taylors' Head Formation. This could help 1) refine the Paleozoic depositional model for the Meguma Supergroup and 2) develop a broader depositional analogue for the offshore Nova Scotia Mesozoic strata. Suggested study locations for the Cunard Formation are the cliff cuttings for the railways tracks in Halifax, and Taylors' Head provincial park for the Goldenville Group. The final recommendation is determining if ichnofossils exist in these outcrops. There are imprints on the surface of some of the outcrops that look like *Cruziana* ichnofossils. Furthermore, trace fossils attributed to a horizontal grazing worm was discovered on some of the blocks (Tobey 2004), however no burrows have been observed since. An ichnofossils study could assist in refining the depositional environment interpretation.

The results suggest these outcrops are a good depositional analogue for low density turbidite deposits. This is useful as other examples of levee and overbank deposits are found as cores, which are very expensive to produce with a small area to observe, and no lateral continuity.

6. References

Basu, D. and Bouma, A.H, 2000, Thin-bedded turbidites of the Tanqua Karoo: physical and depositional characteristics, *in* A.H. Bouma and C.G. Stone, eds., Fine-grained turbidite systems, AAPG Memoir 72/SEPM Special Publication No. 68, p. 263-278.

Bouma, Arnold H., 1962, Sedimentology of some Flysch deposits: A graphic approach to facies interpretation, Amsterdam: Elsevier, 168 p.

Harris, I., Schenk, P.E,1975, 1975 Field Trip; Ancient Sediments of Nova Scotia. Marine Sediments p 1-119.

Jamieson, B., (2009) Geological map of Halifax, Nova Scotia after White, C.E, Bell J.A., Macleish, D.F., MacDonald, M.A., Goodwin, T.A., MacNeil, J.D., 2007. Geology of the Halifax Regional Municipality, Central Nova Scotia. Report of Activities, NSDNR, pp 125-139.

Kirscher, R.H., Bouma, A.H., 2000, Characteristics of a distributary channel-levee-overbank system, Tanqua Karoo, *in* A.H. Bouma and C.S. Stone, eds., Fine-grained turbidite systems, AAPG Memoir 72/SEPM Special Publication No. 68, p 233-244.

Lowe, D.R, 1982, Sediment gravity flows: II. Depositional models with special reference to the deposits of high-density turbidity currents. Journal of Sedimentary Petrology. **52**, p 279-297.

Mitchum, R.M., Wach, G.D., 2002, Niger Delta Pleistocene Leveed-Channel Fans: Models for Offshore Reservoirs. 22nd Annual Gulf Coast Section SEPM foundation. p. 713-728

Nickerson. J., 2009. ILRIS 3D Parser 5.0.0.3 Instruction Manuel, Dalhousie University, Basin and Reservoir lab, p 1-6

Nickerson. J., 2009. ILRIS 3D System Setup Manuel. Dalhousie University, Basin and Reservoir lab, p 1-12.

Piper D.J.W., 1978, Turbidite muds and silts on deep sea fans and abyssal plains in Sediments in submarine canyons, fans, and trenches (ed. By C.J. Stanley and G. Kelling), pp 163-175.

Piper D.J.W, Noftall, R., Pe-Piper, G., 2010, Allochthonous prodeltaic sediments facies in the Lower Cretaceous at the Tanallon M-41 well: Implications for the deep-water Scotian Basin. AAPG Bulletin, V.94, No.1 (January 2010), pp 87-104.

Point Pleasant Park (N.A.) Retrieved from http://www.pahs.ednet.ns.ca/PPP/ on October 15, 2009

Pratt, B. R., and Waldron, J. W. F., 1991, A Middle Cambrian trilobite faunule from the Meguma Group of Nova Scotia: Canadian Journal of Earth Science, v. 28, p. 1843–1853.

Ryan, R. J., Fox, D., Horne, R. J., Corey, M. C. and Smith, P. K. 1996: Preliminary stratigraphy of the Meguma Group in Central Nova Scotia; *in* Minerals and Energy Branch, Report of Activities 1996, eds.D. R. MacDonald and K. A. Mills; Nova Scotia Department of Natural Resources, Report ME 1996-1, p. 27-34.

Roberts, Comapani, 1994, Structural Control on Tertiary Deep Water Deposition in the Northern Gulf of Mexico, GCSSEPM Foundation 15th Annual Research Conference Submarine Fans and Turbidite systems.

Scallion K.L., 2010, Contamination of Plutons by Manganiferous Country Rock in the Governor Lake Area, North-Central Meguma Terrane, Nova Scotia, M.Sc. Thesis Abstract, Dalhousie University

Schenk, R.J., 1970. Regional variation of the flych-like Meguma Group (lower Paleozoic) of Nova Scotia compared to Recent sedimentation off the Scotian Shelf, *in* Lajoie,J., ed., Flych sedimentary in North America: Geological Association of Canada Special Paper 7, p 127-153.

Schenk, P.E. (1997) Sequence stratigraphy and provenance on Gondwana's margin: The Meguma zone (Cambrian–Devonian) of Nova Scotia, Canada: Geological Society of America Bulletin, 109, pp. 395–409.

Scott, D.B. (2003), Foraminifera for the Cambrian of Nova Scotia. Paleontology p 127

Schwarz, E., Arnott R.W.C., 1997, Outcrop characterization of a passive-margin channel complex set: Isaac channel 5, Neoproterozoic Isaac Formation, British Columbia, Canada in T.H. Nilsen, R.D. Shew, G.S. Steffens, and J.R.J. Studlick, eds., Atlas of deep-water outcrops: AAPG Studies in Geology 56, CD-ROM, 15p.

Slatt, R.M., Weimer. P, Stone, C.G. 1997. Reinterpretation of Depositional Processes in a Classic Flych Sequence (Pennsylvanian Jackfork Group), Ouachita Mountains, Arkansas and Oklahoma: Discussion. AAPG Bulletin, V. 81 No. 3 (March 1997), p 449-459.

Stelting, C.E. A.H. Bouma, and C.G Stone, 2000, Fine-grained turbidite systems: overview, in A.H. Bouma and C.S. Stone, eds., Fine-grained turbidite systems, AAPG Memoir 72/SEPM Special Publication No. 68, p1-8.

Stow, D.A.V., Shanmugam, G., 1980, Sequence of structures in fine-grained turbidites; comparison of recent deep-sea and ancient flych sediments. Sedimentary Geology, **25**, 23-42

Stow, D. A. V., Alam, M., and Piper, D. J. W., 1984, Sedimentology of the Halifax Formation, Nova Scotia: Lower Palaeozoic fine-grained turbidites, *in* Stow, D. A.V., and Piper, D. J.W., eds., Fine-grained sediments: Deep water processes and facies: Geological Society of London Special Publication 15, p. 127–144.

Tobey,N., 2004, Geological Description of Point Pleasant Park, B.Sc. Honours Thesis, Dalhousie University.

Wach, G.D., T.C Lukas, R.K. Goldhammer, H. deV. Wickens, and A.H. Bouma, 2000, Submarine fan through slope to deltaic transition basin-fill succession, Tanque Karoo, South Africa, in A.H. Bouma and C.S. Stone, eds., Fine-grained turbidite systems, AAPG Memoir 72/SEPM Special Publication No. 68, p 173-180.

Waldron, J.W.F., Chris E. White, Sandra M. Barr, Antonio Simonetti, and Larry M. Heaman, 2009, Provenance of the Meguma terrane, Nova Scotia: rifted margin of early Paleozoic Gondwana, Can. J. Earth Sci. 46(1), p1–8.

Waldron J.W.F, 2010, Megumia...? Ideas on the provenance of the Meguma Terrane Abstract, DIRT Seminar, Dalhousie University

Walker, R.G., James, N.P., 1992, Facies Models: Response to Sea Level Change, Geological Association of Canada, p. 1-375.

White, C.E, Bell J.A., Macleish, D.F., MacDonald, M.A., Goodwin, T.A., MacNeil, J.D., 2007. Geology of the Halifax Regional Municipality, Central Nova Scotia. Report of Activities, NSDNR, pp 125-139.

Appendix 1
Auslog Methodology

AUSlog Methodology and Procedure

<u>Purpose</u>
The AUSlog is used to record the gamma ray count in a lithology which can be plotted into a well log.

<u>The equipment</u>
1. AUSlog
2. PDA
3. Batteries

<u>PDA</u>
1. Open the GeoGamma2 and create a new folder for the outcrop. The new folder will automatically save any information that was recorded.
2. The PDA should show a chart, and the number of counts. The chart be left on or changed it to RECORD with VIEW on the bottom of the screen. This screen will show the name of the folder, the number of counts recorded, and the average gamma ray count over a certain amount.
3. On the bottom right of the screen is says SETTINGS. Click on the tab and click on ACQUISTION. The tab has a box in the middle called SELECT SAMPLING PERIOD . The choices for sampling are 1, 10, and 30 seconds. For accurate recordings, choose 10 or 30 seconds.
4. Go back to RECORD under VIEW and push SAMPLE. Turn on the AUSlog and start recording. To stop recording just push the stop button. This will stop recording, but the AUSlog will keep showing different gamma ray recordings.

<u>Importing the records into the PC</u>
1. Attach the PDA to the computer
2. On the bottom left of the PDA there is a tab saying FILE, where there is a tab to EXPORT.
3. After tapping EXPORT, the file name, and a folder which the data will import in. The data will automatically choose CSV. When the computer is opened, the data will appear on the computer as a spreadsheet.
4. Find the folder on the computer.

Appendix II
LiDAR and LiDAR software

LiDAR and Software Methodology

<u>Use</u>

The LiDAR is use to scan objects and structures into point clouds. The point clouds can be used to interpret data such as architectural elements or to make geomodels and reservoir models. This section will focus on the using the machine, and how to develop it into an image.

<u>Equipment needed</u>

1. ILRIS-HD scanner

2. PAN-TILT (if needed)

3. Batteries

4. Tripod

5. Cables

1. Ethernet cord

2. PAN-TILT cables

3. USB stick

4. Portable computer or PDA

5. Antenna

ILRIS-HD machine with PAN-TILT

1. Attach PAN-TILT to Tripod. Try to make the Tripod as horizontal as possible. There is an H at the bottom of the PAN-TILT, and this H should be pointed away from what is going to be scanned.
2. There is a lock on the side of the PAN-TILT. Pull this lock outwards. This causes the circles on the top to move. Put the ILRIS-HD on top of the PAN-TILT and close to the lock to set the ILRIS-HD in place.
3. Attach PAN-TILT cables to PAN-TILT and ILRIS-HD scanner, and powercord to PAN-TILT and batteries.

PAN-TILT cable

Powercord socket

4. Insert USB stick and antenna into ILRIS-HD, and turn on ILRIS-HD

ILRIS-HD machine without PAN-TILT

1. Attach ILRIS-HD to Tripod.
2. Attach powercord to ILRIS-HD and batteries
3. Insert USB stick and antenna ILRIS-HD, and turn on ILRIS-HD

Toughbook

1. Open up the program and go to TOOLS where there are camera settings. Change the settings to cloudy so the image taken will be clearer and brighter.
2. Push the image button on the bottom right of the screen. The button has 3 squares coloured red, green, and blue. This will make the ILRIS-HD either take a 360 scan of the area if one is using PAN-TILT or one image with no PAN-TILT.
3. When the scan is done, a green square will appear.
   This green square will highlight were the ILRIS-HD will scan. Expand the square and move it to your desired area for scanning.

4. Choose the size of scanning. This will also tell how long it will take to scan the image in that detail.
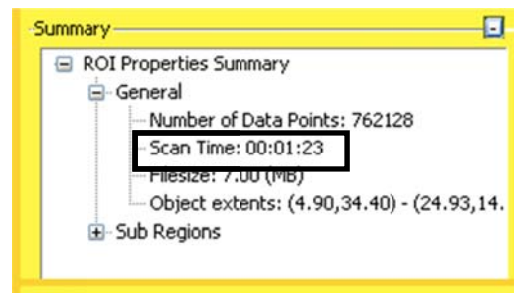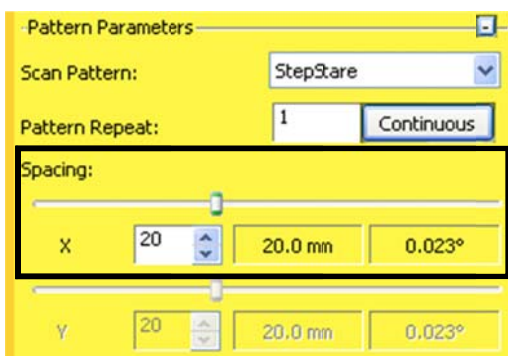
5. Make a folder for the scan to be put into and then push scan.

<u>PDA</u>

1. The process is the same but on the PDA but the PDA has > on the sides so one just has to follow the arrows and complete the information like file and scan size.

<u>Parser</u>

1. Open up Parser and import ILRIS-HD file.
2. Open SETTINGS, click on PANTILT TRANSFORM, and click on APPLY PAN-TILT TRANSFORM (STATIC MODE)
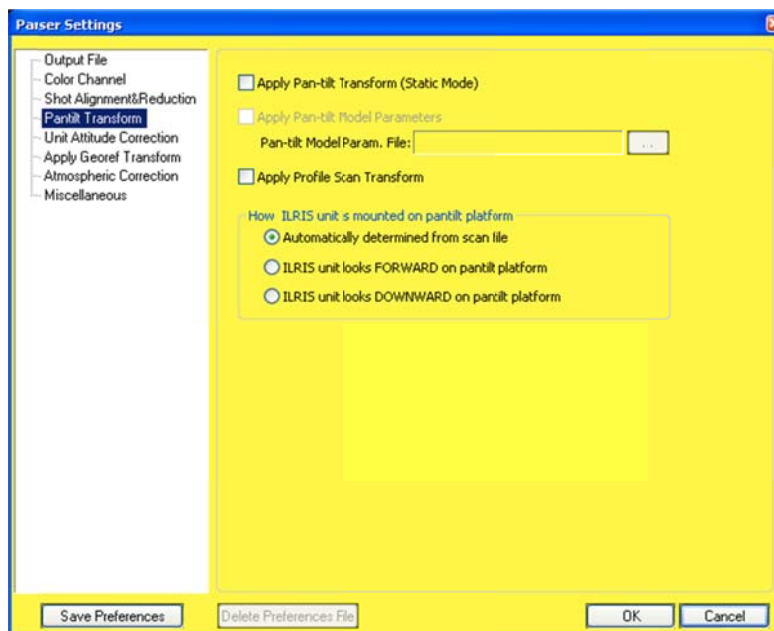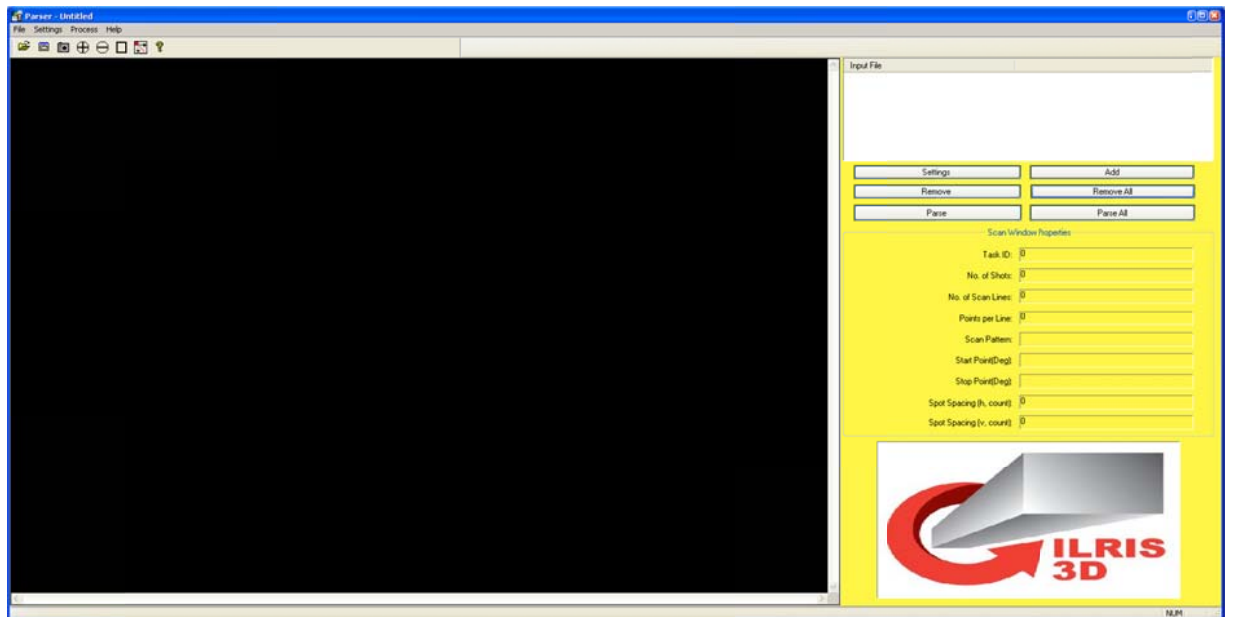
3. Click on OUTPUT FILE and choose XYZ FILE. This will save the file as a xyz file
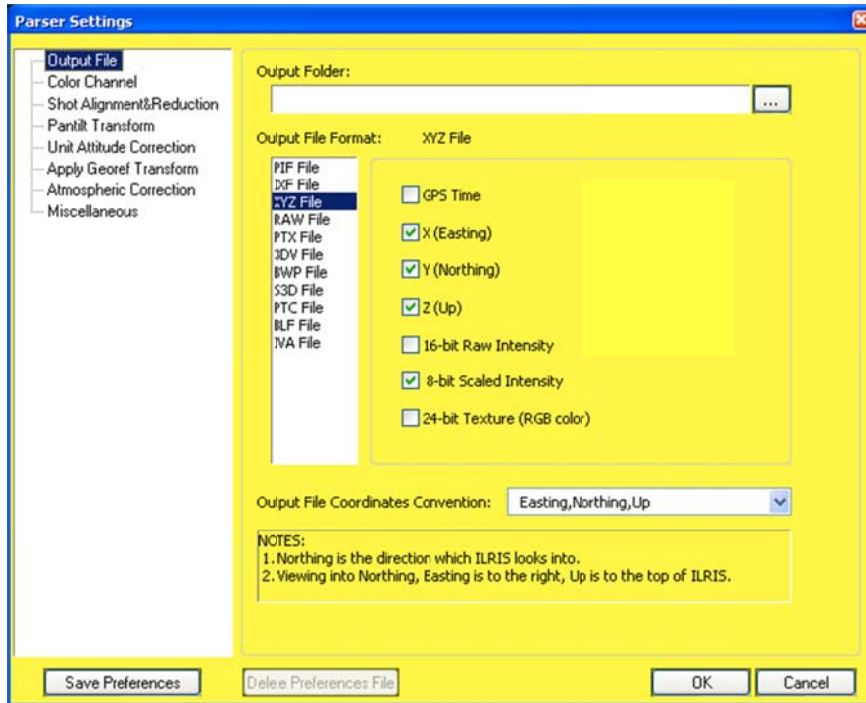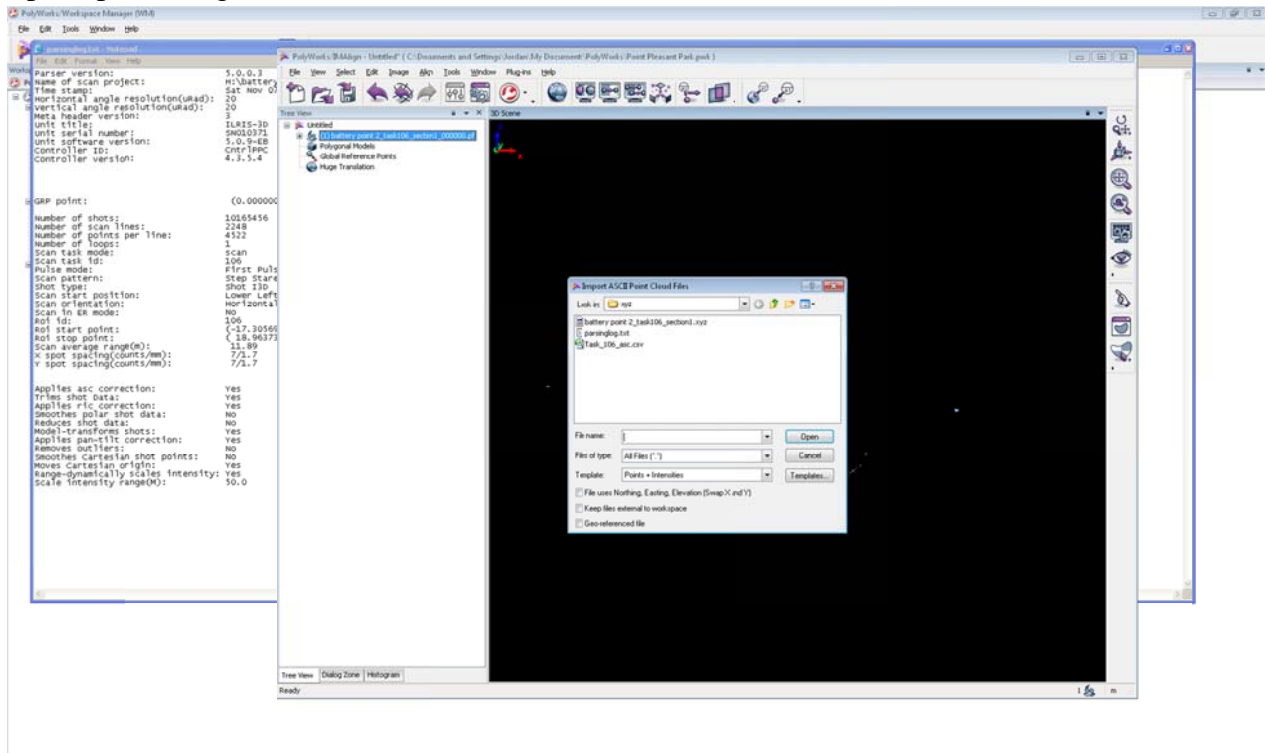
4. Go back to the main screen and push PARSE
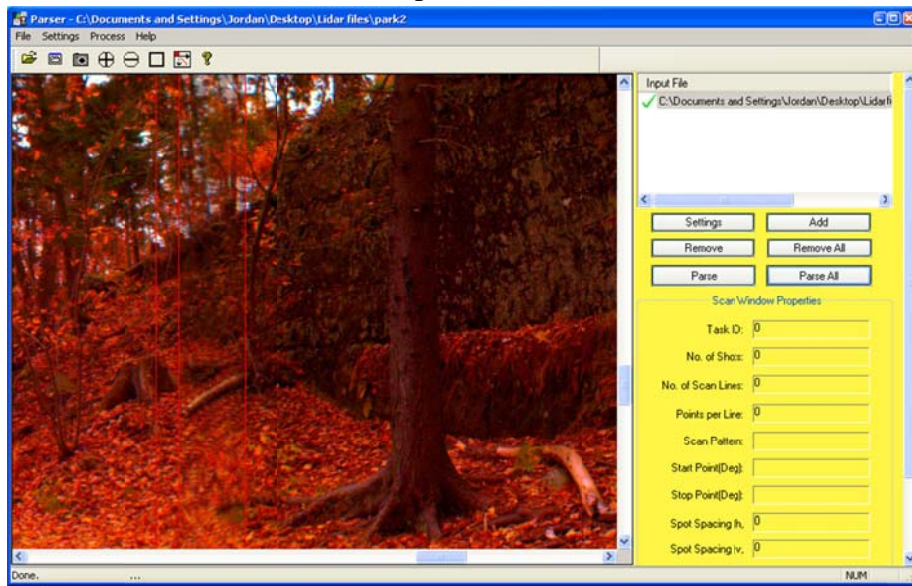
PolyWorks

1. Open up the IMALIGN, open the IMPORT IMAGES , choose POINT CLOUD INTO TEXT FILE, and choose the XYZ file.
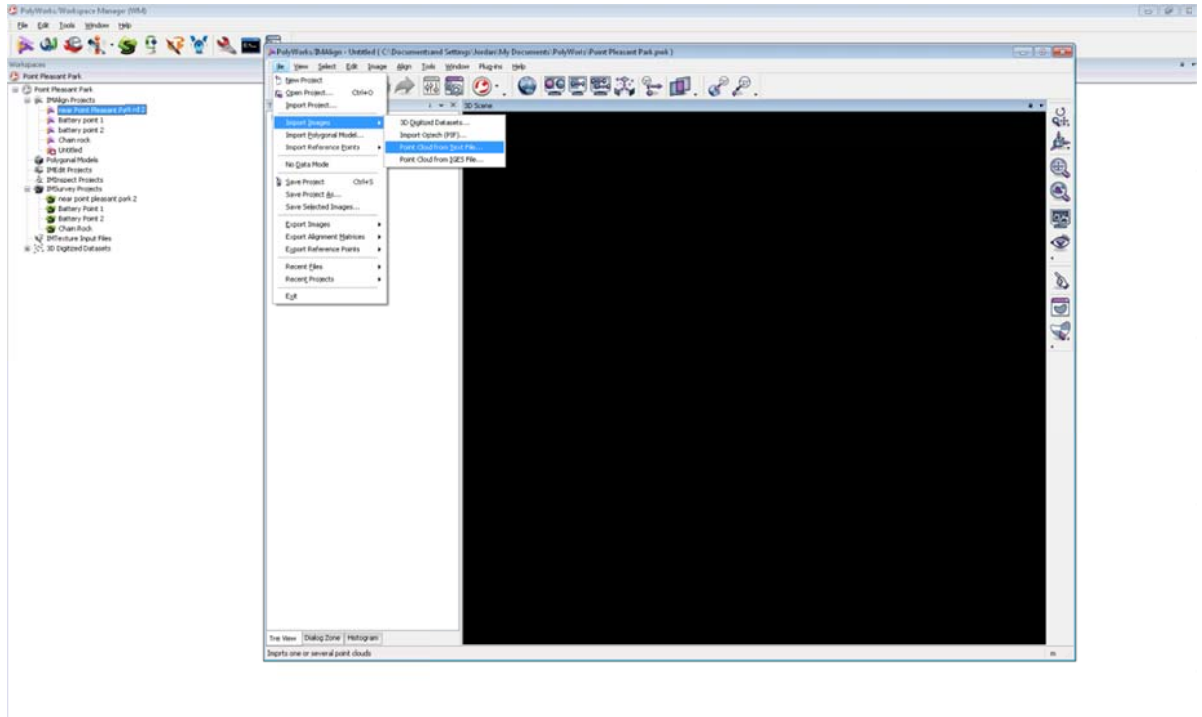
2. Open up the image and show it as POINTS + INTENSITIES under TEMPLATE

3. click OK for meters.
4. Move the image so it is in the right orientation and push ANCHOR
5. Push NEXT STEP. A box will open asking about angles and position. In MAX EDGE LENGTH box change it to 0.5 and leave the MAX ANGLE alone. Open up the xyz file from the scanned image file and open up of the parsinglog. There, the

position can be determined from the second value under X SPOT SPACING. Add the second value into the INTERPOLATION STEP. Push OK when everything is done
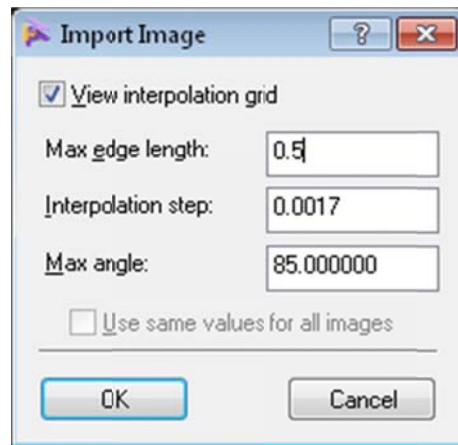
6. Push DONE. This will leave you with a blue image
7. Push the OBJECT DISPLAY OPTIONS, and change the OBJECT COLOR MODE, and DRAWING TYPE to POINT
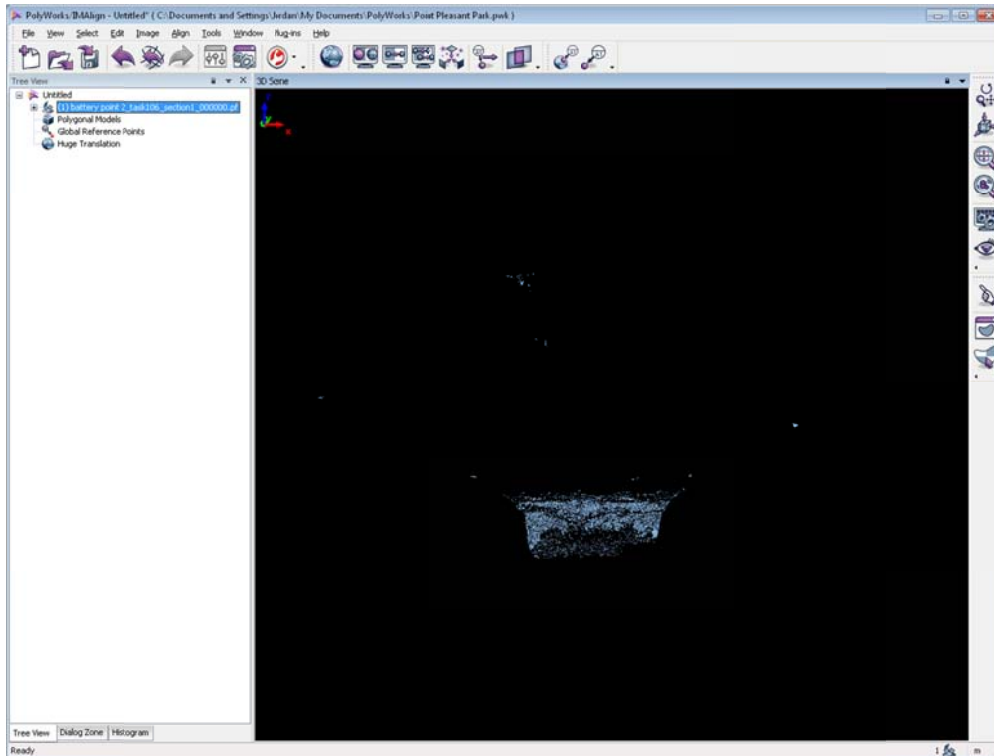
8. Add the saved image to IMSURVEY.

Adding data intro Petrel

1. Open up PETREL 2008 and click OK to the SELECT LICENCE PACKAGE window.

2. Push onto the import file button and it will open up the following window;
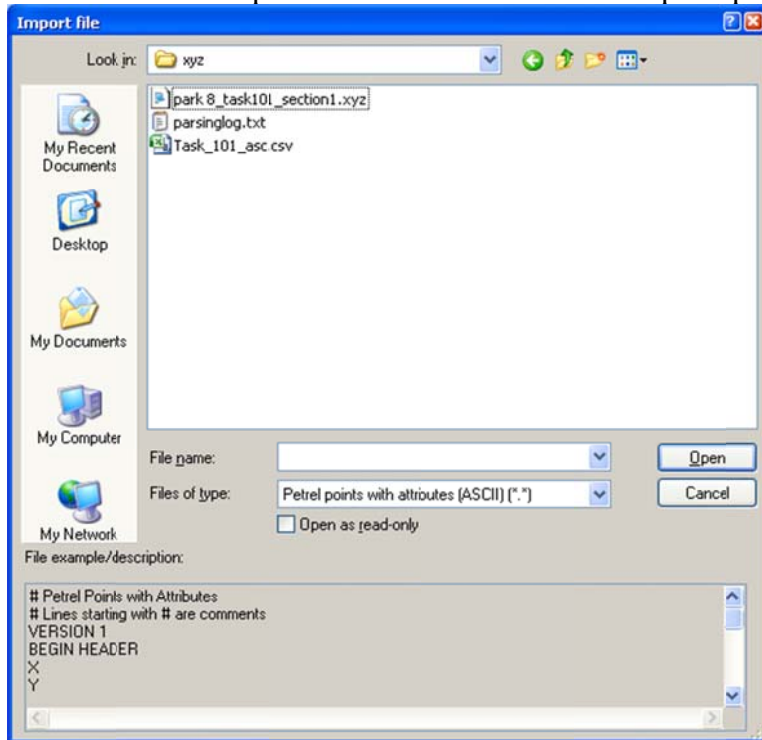
Make sure that the FILE OF TYPE is set to PETREL POINTS WITH ATTRIBUTES. click on the scan you want to import and click OK. If you have multiple files that you import at once, the program will ask to merge these files into one.
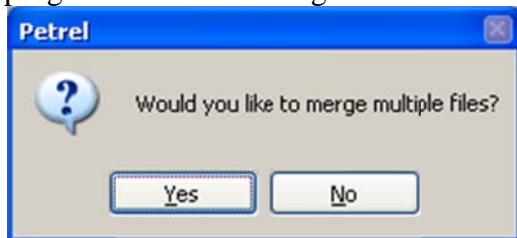
Click YES to this action.

3. The next window verifies that the points have a XYZ position. Click OK TO ALL at the bottom of the next window.

4. On the top right, there is a input column containing the imported LiDar point cloud. Highlight the name and copy the files by doing Ctrl C then pasting by clicking Ctrl V. This will form a copy of the original point cloud.

5. Right click on the copied file and click on SETTINGS. Click on the STYLE tab and change the setting seen in this window:
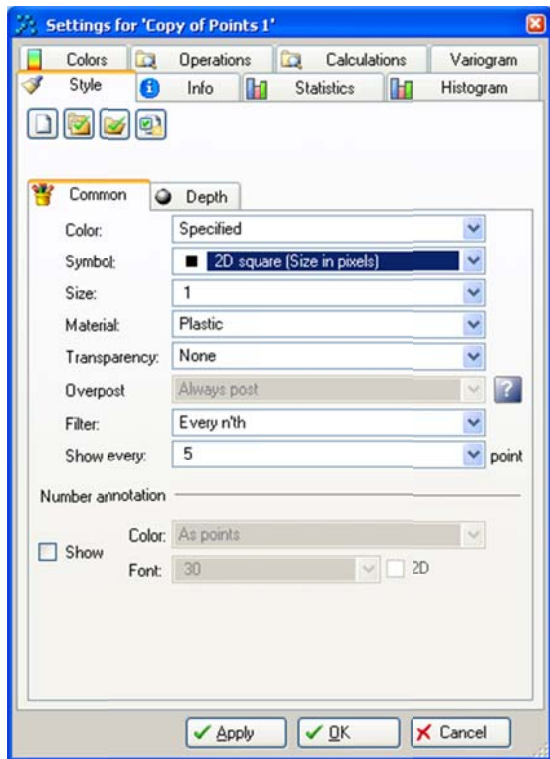
Push APPLY and OK.

6. Right click on the copied point cloud and click on CALCULATOR. Enter in to the task bar; Z=Z*-1 and push ENTER.
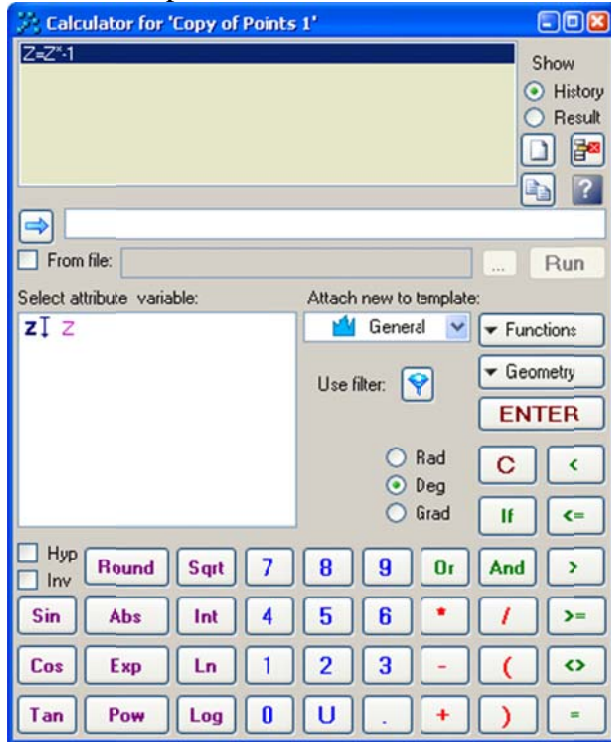

Close the calculator and push on the box next to the copy name.

7. Orientate the image so that it's in its desired location.

8. Finally to fix the scale of the image, change number in this box on the top of the screen [icon].

Deleting points in Petrel

1. Click on WINDOW and click on the 2D window. When the window opens, click on the box next to the copied points.
2. The second column on the left side of the screen contains a series of different processes that can be done on the data. Click on the UTILITIES and click on the MAKE/EDIT POLYGONS.
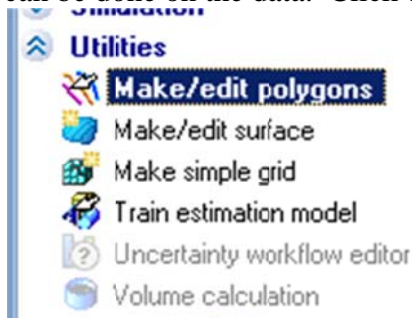

3. Click on the [icon] button to begin a new polygon.
4. Click around the points you want deleted.

5. When polygon is finished, push on the [icon] and [icon] to close and complete the polygon.
6. Right click on the copied points name and click on SETTINGS. Push the OPERATIONS tab and click on the ELIMINATE WHERE file. Click on the ELIMINATE INSIDE file, and drag the polygon found in the side of the input column into the box.
7. Push RUN.
 ATTENTION: this will take a while to complete so if the computer is not responding, its due to the computer deleting the points.

Appendix III
Composite log of the park

Appendix IV
True thickness composite log

Appendix V
Type Section with scintillometer data

Sedimentary Log

(a)

(b)

(c)
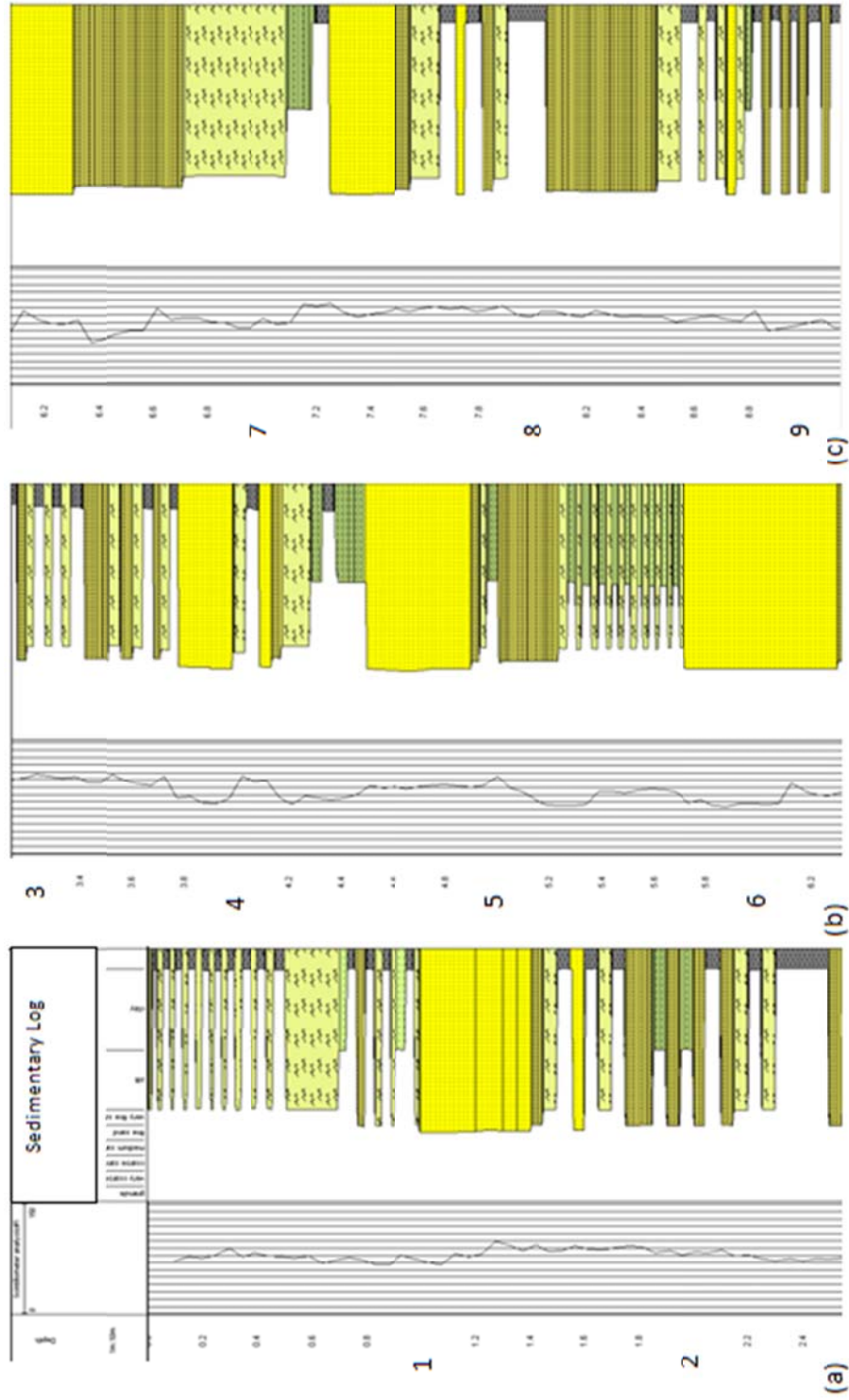
Legend

Structureless hornfels   E

Meta siltstone laminae   D

Meta sandy-siltstone climbing ripples   C

Meta silty-sandstone laminae   B

Structureless meta fine grained sandstone A

(e)

(d)